

UNCLASSIFIED

AD 274 238

*Reproduced
by the*

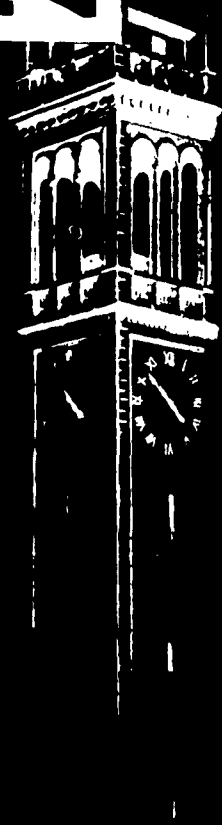
**ARMED SERVICES TECHNICAL INFORMATION AGENCY
ARLINGTON HALL STATION
ARLINGTON 12, VIRGINIA**



UNCLASSIFIED

NOTICE: When government or other drawings, specifications or other data are used for any purpose other than in connection with a definitely related government procurement operation, the U. S. Government thereby incurs no responsibility, nor any obligation whatsoever; and the fact that the Government may have formulated, furnished, or in any way supplied the said drawings, specifications, or other data is not to be regarded by implication or otherwise as in any manner licensing the holder or any other person or corporation, or conveying any rights or permission to manufacture, use or sell any patented invention that may in any way be related thereto.

274 238



274238

AS AD NO.

The Equiangular Plane Spiral Antenna

by
R. Sussman

Series No. 60, Issue No. 406
Contract No. AF 49(638)-1043
September 15, 1961

62-3-1

ELECTRONICS RESEARCH LABORATORY

UNIVERSITY OF CALIFORNIA
BERKELEY CALIFORNIA

AFOSR 2265

Electronics Research Laboratory
University of California
Berkeley, California

THE EQUIANGULAR PLANE SPIRAL ANTENNA

by

R. Sussman

Institute of Engineering Research
Series No. 60, Issue No. 406

Air Force Office of Scientific Research
of the Air Research and Development Command;
Department of the Navy, Office of Naval Research;
and Department of the Army
Contract No. AF 49(638)-1043

September 15, 1961

ACKNOWLEDGMENT

The author wishes to express his sincere gratitude to Prof. Jack Welch for his direction of all phases of the project; to Fred Clapp for his technical assistance and advice; and to his wife Ilana.

SUMMARY

The "Equiangular Plane Spiral Antenna" belongs to the class of "Frequency Independent Antennas," a class which has recently drawn much attention.

In view of the fact that there has not yet been found a solution for the electromagnetic field of the "Equiangular Plane Spiral Antenna" with a finite number of arms, its field is investigated here mainly experimentally. In particular, the pattern, the phase variation and the polarization of the field of spiral antennas with a small number of arms, as generated by various methods of excitation, are examined.

In order to achieve this, a method of decomposing any complicated feeding arrangement into a set of "basic" feedings has been developed. This method is not restricted to spiral antennas, but can be applied also to any equally spaced plane antenna with any number of arms.

Next, measurements on 2-, 4-, and 6-arm spiral antennas have been performed. The results of the measurements show that the solution recently found for the limiting case of a spiral antenna which has an infinite number of arms, can serve as a good approximation to antennas with a small number of arms. Some correction terms, which depend on the number of arms, are introduced into the solution of the "infinite" arm antenna, so as to get a still better approximation.

The combination of the method of decomposition into basic feedings with the experimental results leads to an approximate expression for the field of a spiral antenna, with any number of arms and any feeding arrangement.

TABLE OF CONTENTS

	Page
I. INTRODUCTION	1
II. THEORETICAL CONSIDERATIONS	4
A. The Admittance Matrix	4
B. The Decomposition of the Input Currents into Components	6
C. Analysis of Some Feeding Arrangements	12
D. The Field on the Axis of the Antenna	17
III. THE EXPERIMENTAL WORK	19
A. The Solution for the Field of the Idealized Spiral Antenna	19
B. Some Remarks on the Aims of the Measurements .	22
C. The Measuring Apparatus	23
D. Results of the Measurements on the 2-Arm Spiral Antenna - 2A	26
E. Results of the Measurements on the 4-Arm Spiral Antenna - 4A	27
F. Results of the Measurements on the 4-Arm Spiral Antenna - 4B	28
G. Results of the Measurements on the 4-Arm Spiral Antenna - 4C	30
H. Results of the Measurements on the 6-Arm Spiral Antenna - 6A	31
I. Results of the Measurements on the 6-Arm Spiral Antenna - 6B	31
J. Conclusions	32
IV. CONCLUSIONS	33
A. A Summarized Presentation of the Conclusions . .	33
B. A Detailed Presentation of the Conclusions	33
C. Conclusion	37
REFERENCES	57

LIST OF FIGURES

Figure	Page
1. A four arm spiral antenna	2
2. The terminal currents and voltages	4
3. The coordinate system	10
4. The four arm antenna — 4C	13
5. The six arm antenna — 6B	16
6. The six arm antenna — 6A	16
7. The excitation of the idealized spiral antenna	20
8. The "preferred" sense of polarization	21
9. The arrangement for the phase measurements	24
10. The different regions	24
11. Arrangement for pattern measurements	25
12. The feeding arrangement of the 2A-antenna	26
13. The feeding line coming along the arms	26
14. The feeding arrangement of the 4A-antenna	27
15. The feeding arrangement of the 4B-antenna	28
16. The feeding arrangement of the 4C-antenna	30
17. The feeding arrangement of the 6A-antenna	31
18. The feeding arrangement of the 6B-antenna	32
19. Phase progression of the 2A-antenna	38
20. Pattern of the 2A-antenna	39
21. Pattern of the 2A-antenna	40
22. Phase progression of the 4A-antenna	41
23. Pattern of the 4A-antenna	42
24. Pattern of the 4A-antenna	43
25. Phase progression of the 4B-antenna	44
26. Pattern of the 4B-antenna	45
27. Pattern of the 4B-antenna	46
28. Phase progression of the 4C-antenna	47
29. Pattern of the 4C-antenna	48
30. Pattern of the 4C-antenna	49
31. Phase progression of the 6A-antenna	50

LIST OF FIGURES (cont.)

Figure	Page
32. Pattern of the 6A-antenna	51
33. Pattern of the 6A-antenna	52
34. Phase progression of the 6B-antenna	53
35. Phase progression of the 6B-antenna	54
36. Pattern of the 6B-antenna	55
37. A summarized table of measurements	56

INTRODUCTION

One of the most frequently encountered problems in antenna theory and practice is the design of antennas which present a fairly constant input impedance, and have essentially the same field strength pattern, over as large a range of frequencies as possible. An antenna for which these properties, namely, the input impedance and the pattern, remain constant over a range of frequencies of 1:2, is already considered a wide band antenna. But this band width is still not large enough for many practical uses.

To meet this shortage, a new class of antennas was proposed by V. H. Rumsey,¹ a class which was called the "Frequency Independent Antennas." Two common properties characterize this new class. First, these antennas can be fully described by dimensionless numbers, such as angles or ratios; and second, the total current flowing out of the center of these antennas along their structure decreases rapidly. Consequently, the currents at distances of several wavelengths off the center of the antenna, and further, can be neglected.

The first property would require an antenna of infinite size, as any cutting off of the antenna would introduce a linear dimension, and so contradict our assumptions. It is the second property which allows us to use only the central part of the antenna, and cut off all parts which lie beyond some radius.

To illustrate the importance of the second property, consider the biconnical antenna. It is an example of an antenna for which the first property holds, namely, it is characterized only by angles, but for which the current, through any cross section, remains constant, no matter how far away from the center of the antenna. Thus, not having the second property, it cannot be considered as a frequency independent antenna. This follows from the fact that any termination of the antenna will cause a major change in the field, and particularly, will make the field frequency dependent.

Even though this class of antennas is frequency independent, the practical structure will of course have a finite frequency range, but very much larger than the so-called "wide-band" antennas. The frequency range may be of the order of 1:20!

The low frequency limit of these antennas is determined by the over-all size of the antenna; whereas the high frequency limit is due to the fact that the feeding line cannot be made infinitely small, as well as due to the structural irregularities of the antenna.

One of the groups of antenna that belong to the class of frequency independent antennas is the group of the "Plane Equiangular Spiral Antennas." An equiangular spiral can be described in polar coordinates by the function

$$\rho = e^{-a(\phi - \phi_0)} \quad (1.1)$$

Note that none of the constants a or ϕ_0 has the dimension of length. An antenna which is made of conducting arms, the contours of which are equiangular spirals, is called a "Plane Equiangular Spiral Antenna."

The antennas considered in this thesis will always have equally spaced arms, and will be self-complementary.* The number of the arms may range from one to infinity.

These "Multiarm, Plane, Self-complementary, Equiangular Spiral Antennas" will be called from now on simply, "Spiral Antennas."



Fig. 1. --A four arm spiral antenna

* Two structures are called complementary, if one is obtained from the other by exchanging the open and conducting portions of the plane. If these two structures are equivalent, except for a rotation by some angle around their center, each one of these structures is said to be self-complementary.

In contrast to the input impedance and the pattern, ** the phase distribution is affected by variations of the frequency. A consideration of (1.1) will show that any variation of the frequency will be accompanied by a rotation of the field around the axis of the antenna. If, for example, the wave length λ is increased, also ϕ will have to increase, so as to keep ρ/λ constant. In other words, the effect of multiplying ρ by some constant, is the same as increasing the angle ϕ . That is,

$$K_{\rho} = Ke^{-a(\phi - \phi_0)} = e^{-a} e^{-a(\phi - \phi_0)} = e^{-a[(\phi + \frac{a}{a}) - \phi_0]}$$

An exact solution for the electro-magnetic field has recently been found for an antenna which may be called the "Idealized Spiral Antenna."² This antenna can be considered as a limiting case of the spiral antenna when the number of the arms tends to infinity. Actually, this antenna could as well be described as an unisotropically conducting sheet, which has a conductivity only in the direction of the spirals. The antenna was assumed to extend to infinity. Unfortunately, no exact solution has yet been found for the general case of any finite number of arms.

The purpose of this work is to investigate, mainly experimentally, the properties of the spiral antenna with a small number of arms, under various feeding arrangements. The feeding arrangement will mean here the different methods of connecting the feeding line (or lines) to the arms of the antenna, as well as the interconnections among the arms at the center of the antenna. Particularly, the investigation is carried on so as to find out how far can the exact solution,

** The plane for which the pattern remains constant when the frequency is varied actually rotates around the axis of the antenna. However, if the spirals are "tight" enough, the pattern in all planes through the axis of the antenna will be very similar for all frequencies in the range of the "frequency independent" operation of the antenna.

which has been found for the idealized spiral antenna, be applied to the spiral antenna which has a small number of arms.

The second chapter will contain some conclusions that can be derived from theoretical considerations. In the third chapter a resumé of the experimental work done will be presented. Then, in the fourth chapter, an essay will be made to connect the theoretical considerations, derived in Chapter II, together with the experimental results, in order to get an understanding of the performance of the spiral antenna.

II. THEORETICAL CONSIDERATIONS

This chapter will deal with the general case of an equally spaced, self-complementary antenna, with any number of arms. The shape of the arms is not specified and may be of any form. All the results obtained in this chapter are based only upon considerations of symmetry. More specifically, no attempt will be made to solve Maxwell's equation, and thus to find the electro-magnetic field of the antenna; but still several important features of the electro-magnetic field can be derived from a purely geometrical point of view, by an examination of the symmetry of the antenna.

A. The Admittance Matrix

Consider an equally spaced, self-complementary, n -arm antenna; the shape of the arms may be of any form.

In the center of the antenna, a circle of radius r is excluded from the antenna, and will be the feeding zone of the antenna.

As long as $r \ll \lambda$

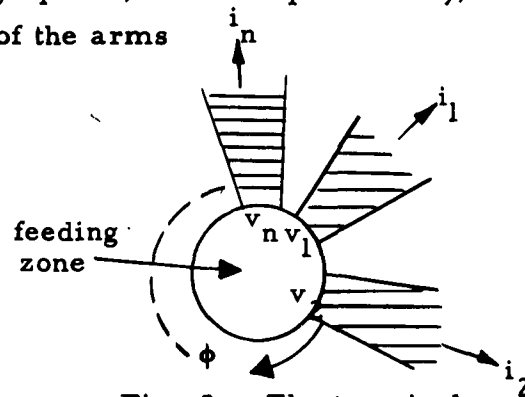


Fig. 2. -- The terminal currents and voltages

(λ - the wavelength), this circle may be treated from the point of view of low-frequency circuit analysis, i. e., the n -conductors at the circle can be regarded as terminals of an n -terminal network, assuming that the antenna is placed in an isotropic medium.

In consequence, the current and voltage relations can be described as in circuit analysis, in terms of the usual admittance matrix.

The voltages v_1, v_2, \dots, v_n , may be measured with reference to any fixed voltage. The currents i_1, i_2, \dots, i_n are taken to be positive when flowing out of the circle. The only restriction on the currents is that $i_1 + i_2 + \dots + i_n = 0$ as imposed by Kirchhoff's law.

De Champs,³ expanding Booker's⁴ theorem on the admittance of complementary planes, has found that the admittance matrix of the equally spaced self-complementary antenna has the following form:

$$\begin{bmatrix} i_1 \\ i_2 \\ \cdot \\ \cdot \\ \cdot \\ \cdot \\ i_{n-1} \\ i_{n-2} \end{bmatrix} = \begin{bmatrix} y_0 & y_1 & y_2 & \cdot & \cdot & \cdot & y_{n-1} \\ y_{n-1} & y_0 & y_1 & \cdot & \cdot & \cdot & y_{n-2} \\ \cdot & \cdot & \cdot & \cdot & \cdot & \cdot & \cdot \\ \cdot & \cdot & \cdot & \cdot & \cdot & \cdot & \cdot \\ \cdot & \cdot & \cdot & \cdot & \cdot & \cdot & \cdot \\ \cdot & \cdot & \cdot & \cdot & \cdot & \cdot & \cdot \\ y_2 & y_3 & y_n & \cdot & \cdot & \cdot & y_1 \\ y_1 & y_2 & y_3 & \cdot & \cdot & \cdot & y_0 \end{bmatrix} \begin{bmatrix} v_1 \\ v_2 \\ \cdot \\ \cdot \\ \cdot \\ \cdot \\ v_{n-1} \\ v_n \end{bmatrix} \quad (2.1)$$

where all the elements of the matrix are given by the formula:

$$y_i = \frac{4\eta}{n} \cdot \frac{\cos \theta/2}{\cos i\theta - \cos \theta/2} \quad i = 0, 1, 2, \dots, n-1 \quad (2.2)$$

where

n - number of arms,

$$\theta = \frac{2\pi}{n}$$

$$\eta = \sqrt{\frac{\mu}{\epsilon}} \cong 377\Omega \text{ in free space.}$$

These works were based on Babinet's principle, generalized to electromagnetism, which gives a relation between the incident and the scattered field of a complementary plane structure.

Note that as this admittance matrix is symmetric, it will include $\frac{n}{2} + 1$ different elements for an even number of arms, and $\frac{n+1}{2}$ different elements for an odd number of arms.

Thus for any arrangement of passive and active elements in the feeding zone, all input currents and terminal voltages can be calculated in terms of this admittance matrix.

B. The Decomposition of the Input Currents into Components

Applying the results of the previous section, we are able to compute all the currents and voltages at the terminals of the antenna, in terms of the feeding sources connected between the terminals. Following a method suggested by Dyson,⁵ the input currents will be decomposed into components which have some symmetry. These components will be called the "characteristic feedings". It will be shown that the electro-magnetic field obtained from each of these characteristic feedings will also have some kind of symmetry. Specifically, the results of this analysis will direct us, when representing the field in a Fourier series, as to which terms of the series may be excluded.

First, the method of decomposing the input currents will be developed.

It will be convenient to express the input currents in a vector form,

$$I = (i_1, i_2, \dots, i_i, \dots, i_n)$$

where i_i is the current entering into the i -th arm. This vector will be written sometimes horizontally and sometimes vertically.

Any combination of input currents can be expressed as a linear combination of any $n-1$ fixed current vectors, which are linearly independent,

$$\begin{bmatrix} i_1 \\ i_2 \\ \cdot \\ \cdot \\ \cdot \\ \cdot \\ i_\ell \\ \cdot \\ \cdot \\ \cdot \\ i_n \end{bmatrix} = {}^n a_1 \begin{bmatrix} i_{11} \\ i_{12} \\ \cdot \\ \cdot \\ \cdot \\ \cdot \\ i_{1\ell} \\ \cdot \\ \cdot \\ \cdot \\ i_{1n} \end{bmatrix} + {}^n a_2 \begin{bmatrix} i_{21} \\ i_{22} \\ \cdot \\ \cdot \\ \cdot \\ \cdot \\ i_{2\ell} \\ \cdot \\ \cdot \\ \cdot \\ i_{2n} \end{bmatrix} + \dots + {}^n a_{n-1} \begin{bmatrix} i_{n-1,1} \\ i_{n-1,2} \\ \cdot \\ \cdot \\ \cdot \\ \cdot \\ i_{n-1,\ell} \\ \cdot \\ \cdot \\ \cdot \\ i_{n-1,n} \end{bmatrix}$$

(2.3)

where ${}^n a_1, {}^n a_2, \dots, {}^n a_i, \dots$ are complex constants, and all current vectors are subject to the condition: -

$$i_{i1} + i_{i2} + \dots + i_{i\ell} + \dots + i_{in} = 0$$

The decomposition enables us to describe the field excited by any current vector, as a linear combination of $n-1$ fields, excited by any $n-1$ independent fixed current vectors.

Let the n -characteristic vectors of the matrix P_n ,

$$P_n = \begin{bmatrix} 0 & 1 & 0 & 0 & \dots & 0 \\ 0 & 0 & 1 & 0 & \dots & 0 \\ 0 & 0 & 0 & 1 & \dots & 0 \\ \vdots & & & & & \\ \vdots & & & & & \\ 1 & 0 & 0 & 0 & \dots & 0 \end{bmatrix} \quad (2.4)$$

which is of rank n , be denoted by ${}^n I_1, {}^n I_2, \dots, {}^n I_i, \dots$

Solving the matrix P_n for the characteristic vectors we get:

$$\begin{aligned} {}^n I_1 &= (1, e^{j \frac{2\pi}{n}}, e^{j \cdot 2 \cdot \frac{2\pi}{n}}, \dots, e^{j(n-1) \frac{2\pi}{n}}) \\ &\vdots \\ {}^n I_i &= (1, e^{j \cdot i \cdot \frac{2\pi}{n}}, e^{j \cdot i \cdot 2 \cdot \frac{2\pi}{n}}, \dots, e^{j \cdot i(n-1) \frac{2\pi}{n}}) \quad (2.5) \\ &\vdots \\ {}^n I_{n-1} &= (1, e^{j(n-1) \frac{2\pi}{n}}, e^{j(n-1) \cdot 2 \cdot \frac{2\pi}{n}}, \dots, e^{j(n-1)(n-1) \frac{2\pi}{n}}) \\ {}^n I_n &= (1, 1, 1, \dots, 1) \end{aligned}$$

or generally, the l -th term of the i -th vector will be,

$$i_{ie} = e^{j \cdot i \cdot l \cdot \frac{2\pi}{n}} \quad j = \sqrt{-1}$$

Their characteristic value will be denoted by ${}^n \lambda_i$,

and is given by

$${}^n \lambda_i = e^{j \cdot i \cdot \frac{2\pi}{n}} \quad (2.6)$$

These characteristic vectors will be thought of as current vectors which feed an n -arm antenna, and will be the characteristic feedings mentioned above. But note that only the first $n-1$ characteristic vectors can be associated with a current vector, as the n -th vector does not agree with Kirchhoff's law. Namely,

the sum of all the terms of ${}^n I_n$, obviously does not equal to zero.

It will be understood that $1 \leq i \leq n-1$, and also that

$${}^n I_i = {}^n I_{i+np}$$

where p is a positive or negative integer.

The advantage of using these characteristic feedings will be explained now.

For any current vector

$$P_n \begin{bmatrix} i_1 \\ i_2 \\ \vdots \\ i_n \end{bmatrix} = \begin{bmatrix} i_2 \\ i_3 \\ \vdots \\ i_1 \end{bmatrix} \quad (2.7)$$

as can be seen by performing the multiplication. This shows that P_n , when operating upon a current vector, has the property of shifting the input currents by one arm. Or, if we introduce spherical coordinates, and place the antenna in the $\theta = \frac{\pi}{2}$ plane (Fig. 3), the input currents can be expressed as a function of ϕ . So now the shifting property of the matrix may be written as:

$$P_n {}^n I(\phi) = {}^n I\left(\phi + \frac{2\pi}{n}\right)$$

And particularly this is true for any characteristic feeding ${}^n I_i$.

But for any characteristic vector

$$P_n {}^n I_i = {}^n \lambda_i {}^n I_i$$

so that ${}^n \lambda_i {}^n I_i(\phi) = {}^n I_i\left(\phi + \frac{2\pi}{n}\right)$ (2.8)

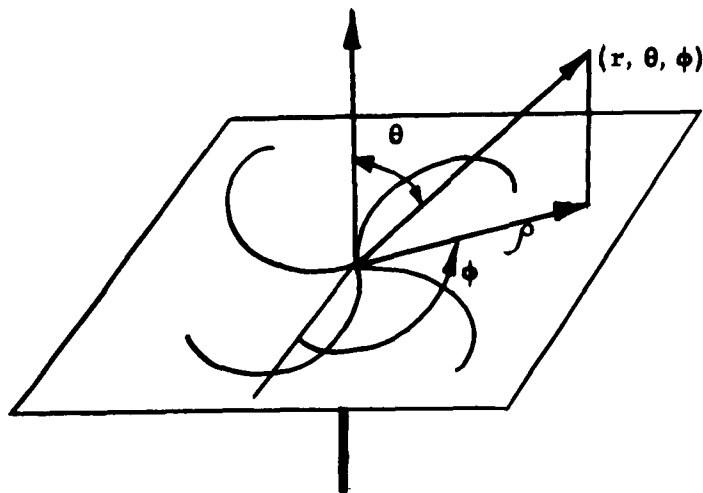


Fig. 3. --The coordinate system

Let ${}^n F_i(r, \theta, \phi)$ be one of the two regular Herz-Potential* functions, which are excited by the i -th characteristic feeding of an n -arm antenna. As the structure of the antenna is periodic in ϕ , with the period $\frac{2\pi}{n}$, a shift of the angle ϕ in ${}^n F_i(\phi)$ will result in a similar shift in the Herz-Potential function. To express this analytically,

$$\frac{{}^n F_i(\phi)}{{}^n F_i(\phi + \frac{2\pi}{n})} = \frac{{}^n F_i(\phi)}{{}^n F_i(\phi + \frac{2\pi}{n})} \quad (2.9)$$

Inserting this result into equation (2.8), we get,

$${}^n \lambda_i {}^n F_i(r, \theta, \phi) = {}^n F_i(r, \theta, \phi + \frac{2\pi}{n}) \quad (2.10)$$

According to the theory of the expansion of functions into Fourier series, the following can always be written,

$${}^n F_i(r, \theta, \phi) = \sum_{m=-\infty}^{\infty} {}^n C_m(r, \theta) e^{jm\phi} \quad (2.11)$$

where r , θ and ϕ are the spherical coordinates.

Inserting the expression (2.11) into equation (2.10), and

*By regular Herz-Potential is meant the potential from which the electric field is derived by the following formula;

$$\mathbf{E} = \nabla \times \hat{\mathbf{z}} {}^n F_{i1} + \nabla \times \nabla \times \hat{\mathbf{z}} {}^n F_{i2}$$

where ${}^n F_i$ stands for either ${}^n F_{i1}$ or ${}^n F_{i2}$.

equating terms which have the same phase variations, we get

$${}^n\lambda_i e^{jm\phi} = e^{jm(\phi + \frac{2\pi}{n})} \quad (2.12)$$

which is a condition imposed on m .

Inserting the value of ${}^n\lambda_i$ from (2.6) into (2.12), it follows that

$$m = i + np \quad (2.13)$$

where i refers to the characteristic feeding chosen, n is the number of arms and p is any positive or negative integer.

This result has a great practical importance, as it tells which terms of the Fourier series may be excluded, and still have an exact representation of the field. Consider, for example, a 6-arm antenna with the following input currents:

$$i_1 = i_3 = i_5 = 1 ; i_2 = i_4 = i_6 = -1$$

This is recognized to be the 6I_3 characteristic feeding (see 2.5). Then from (2.13) it follows immediately that the Herz-Potential can be given by the following series:

$$\begin{aligned} {}^6F_3(r\theta, \phi) = & \dots + {}^6C_{-9}(r\theta) e^{-j9\phi} + {}^6C_{-3}(r\theta) e^{-j3\phi} + \dots \\ & + {}^6C_{+3}(r\theta) e^{+j3\phi} + {}^6C_{+9}(r\theta) e^{+j9\phi} + \dots \end{aligned}$$

excluding all the terms for which $m \neq i + np$.

Later on it will be shown that this series converges rapidly, so that this advantage will be still more pronounced, as it will suffice to include only the first, or two first, terms, and neglect all the rest.

The coefficients ${}^na_1, \dots, {}^na_{n-1}$, (2.3), which give us the relative amplitude of the different characteristic feedings present in the current vector nI , can be evaluated in a simple way by noting that the characteristic feedings have the following property:

$$n_{I_i} \cdot n_{I_j}^* = \begin{cases} 0 & \text{for } i \neq j \\ n & \text{for } i = j \end{cases} \quad (2.14)$$

So if

$$n_I = n_{a_1} n_{I_1} + n_{a_2} n_{I_2} + \dots + n_{a_i} n_{I_i} + \dots + n_{a_{n-1}} n_{I_{n-1}}$$

then

$$n_{a_i} = \frac{1}{n} n_I \cdot n_{I_i}^* \quad (2.15)$$

C. Analysis of Some Feeding Arrangements

1. Introduction

In this section three antennas with different feeding arrangements will be analyzed. First, the input impedance and the input currents of these antennas will be found. Then, the input currents will be decomposed into the characteristic feedings, and the relative amplitude of the characteristic feedings will be calculated. In Chapter III these results will be compared with the measurements of the corresponding fields.

In general, the analysis of any feeding arrangement will proceed according to the following steps:

- (a) find the elements of the admittance matrix for the specific antenna (2.2);
- (b) find the input currents of the antenna, using (2.1);
- (c) find the characteristic feedings and their characteristic values (2.5) and (2.6);
- (d) find the coefficients $n_{a_1}, \dots, n_{a_{n-1}}$, which give us the amplitude of the various characteristic feedings (2.15).

In some special cases it will be possible to make some shortcuts in this procedure, as will be shown in the second and the third examples.

2. The four arm antenna - 4C

Consider a four arm antenna in which two opposite arms are fed by a coaxial line close to the center of the antenna while the two remaining arms are connected through resistance R (Fig. 4).

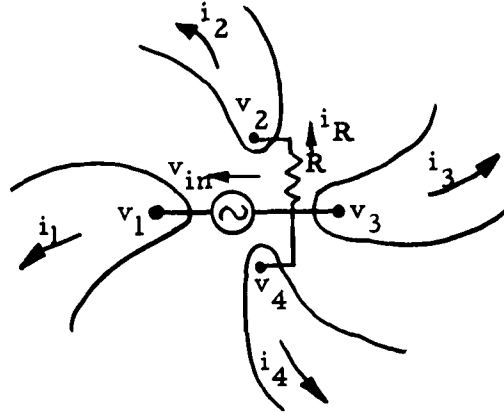


Fig. 4. --The four arm antenna - 4C.

(a) The elements of the admittance are found to be the following:

$$y_0 = \frac{0.707}{1 - 0.707} \cdot \frac{1}{120\pi} = \frac{1}{156} \text{ mho} \quad y_1 = \frac{0.707}{1 - 0.707} \cdot \frac{1}{120\pi} = -\frac{1}{377} \text{ mho}$$

$$y_2 = \frac{0.707}{-1 - 0.707} \cdot \frac{1}{120\pi} = -\frac{1}{910} \text{ mho}$$

(b) The equations (2.16) are the input conditions:

$$\begin{aligned} i_1 = -i_3 = i_{in} & & v_1 - v_3 = v_{in} \\ i_2 = -i_4 = i_R & & v_2 - v_4 = i_R R. \end{aligned} \quad (2.16)$$

In order to find the input currents, these input conditions will be inserted into the admittance-matrix equation (2.1).

$$\begin{aligned} i_{in} &= y_2 v_1 + y_1 v_2 + y_0 v_3 + y_1 v_4 \\ i_{in} &= y_0 v_1 + y_1 v_2 + y_2 v_3 + y_1 v_4 \\ \hline i_{in} &= \frac{1}{2} v_{in} (y_0 - y_2) \end{aligned}$$

Therefore

$$Z_{in} = \frac{2}{y_0 - y_2} = 166 \Omega$$

where Z_{in} is the input resistance to the antenna. Consider the remaining two equations, namely,

$$i_R = y_1 v_1 + y_0 v_2 + y_1 v_3 + y_2 v_4$$

$$-i_R = y_1 v_1 + y_2 v_2 + y_1 v_3 + y_0 v_4$$

$$i_R = \frac{1}{2} R \cdot i_R (y_0 - y_2)$$

and as R can have any value, it follows that $i_R = 0$. Note also that Z_{in} is independent of R .

(c) The shifting matrix for the four arm antenna is,

$$P = \begin{bmatrix} 0 & 1 & 0 & 0 \\ 0 & 0 & 1 & 0 \\ 0 & 0 & 0 & 1 \\ 1 & 0 & 0 & 0 \end{bmatrix}$$

and its three characteristic vectors for which are:

$${}^n I_1 = [1, +j, -1, -j]$$

$${}^n I_2 = [1, -1, 1, -1]$$

$${}^n I_3 = [1, -j, -1, +j]$$

while their characteristic values are:

$${}^n \lambda_1 = +j, \quad {}^n \lambda_2 = -1, \quad {}^n \lambda_3 = -j$$

(d) In (b) the current vector was found to be

$${}^n I = (1, 0, -1, 0)$$

except for a constant multiplier. From formula (2.14) 4a_i will now be calculated.

$$n_{a_1} = \frac{1}{4} n_I n_{I_1}^* = \frac{1}{4} (1, 0, -1, 0)(1, -j, -1, +j) = \frac{1}{2}$$

$$n_{a_2} = \frac{1}{4} n_I \cdot n_{I_2}^* = 0$$

$$n_{a_3} = \frac{1}{4} n_I \cdot n_{I_3}^* = \frac{1}{2}$$

$$\text{so finally: } n_I = \frac{1}{2}(n_{I_1} + n_{I_3})$$

This shows that the field of the antenna considered in this example is equivalent to the sum of the two fields, 4F_1 and 4F_3 , which are excited by the characteristic feedings 4I_1 and 4I_3 respectively.

3. The six arm antenna - 6B

Consider the six arm antenna fed in the way shown in Fig. 5.

From the symmetry of the antenna it can be seen that the current vector will be:

$${}^6I = (1, 0, -1, -1, 0, 1)$$

6I will be composed of the current feedings 6I_1 and 6I_5 . Namely,

$${}^6I = \frac{1}{6}(3 + j\sqrt{3}){}^6I_1 + \frac{1}{6}(3 - j\sqrt{3}){}^6I_5$$

where ${}^6I_1 = [1, e^{j60^\circ}, e^{j120^\circ}, \dots, e^{j180^\circ}, e^{j240^\circ}, e^{j300^\circ}]$

and ${}^6I_5 = [1, e^{j300^\circ}, e^{j240^\circ}, e^{j180^\circ}, e^{j120^\circ}, e^{j60^\circ}]$

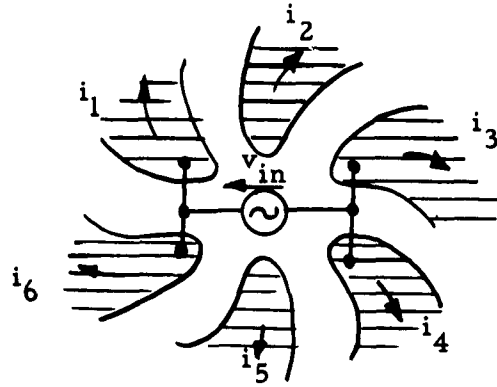


Fig. 5. --The six arm antenna - 6B

4. The six arm antenna - 6A

As a final example consider the six arm antenna when fed in the way shown in Fig. 6.

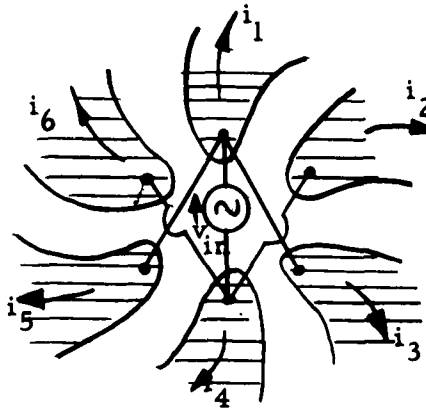


Fig. 6. --The six arm antenna - 6A

From the symmetry of the structure, we can see immediately that the current vector will be:

$${}^6I = (1, -1, 1, -1, 1, -1)$$

but this is exactly the characteristic feeding 6I_3 . So that there is no further need of decomposition.

D. The Field on the Axis of the Antenna

The field on the axis of the antenna is an additional feature, which can also be derived by applying only considerations of symmetry. This will be done only for the case of an antenna fed by one of the characteristic feedings. To find the total field on the axis of the antenna, we have to sum up all the contributions to the field from all the characteristic feedings present in the actual input currents.

Consider an equally spaced, n-arm antenna fed by the characteristic feeding,

$${}^n\mathbf{I}_i = \left[1, e^{j \cdot i \cdot \frac{2\pi}{n}}, e^{j \cdot i \cdot 2 \cdot \frac{2\pi}{n}}, \dots, e^{j \cdot i \cdot (n-1) \frac{2\pi}{n}} \right]$$

Applying again, as in section B, the Fourier series expansion, the electric current density on the antenna at some distance ρ , can be given by the following series:

$$\overline{{}^n\mathbf{J}_i} = \hat{\rho} J_\rho + \hat{\phi} J_\phi = \hat{\rho} \sum_{m=-\infty}^{\infty} a_m(\rho) e^{jm\phi} + \hat{\phi} \sum_{m=-\infty}^{\infty} b_m(\rho) e^{jm\phi}$$

The restriction on m will still be the same as in (2.13), namely, $m = i + p \cdot n$.

In order to find the contribution of each of the current elements to the field on the axis of the antenna, the vector potential A will be calculated. The formula for A is:

$$A = \iint_{\text{over } \overline{{}^n\mathbf{J}_i}} \frac{\mu}{2\pi} \cdot \frac{\overline{{}^n\mathbf{J}_i} e^{-jkr}}{r} \cdot \rho \cdot d\rho \cdot d\phi$$

Now, breaking $\overline{{}^n\mathbf{J}_i}$ into two rectangular components, and performing the integration, we get:

$$A_x = \sum_{m=-\infty}^{\infty} \int_0^{\rho} \int_0^{2\pi} \frac{\mu}{2\pi} \frac{e^{-jkr}}{r} \rho [a_m(\rho) e^{jm\phi} \sin m\phi + b_m(\rho) e^{jm\phi} \cos m\phi] d\rho d\phi$$

$$A_y = \sum_{m=-\infty}^{\infty} \int_0^{\rho} \int_0^{2\pi} \frac{\mu}{2\pi} \frac{e^{-jkr}}{r} \rho [a_m(\rho) e^{jm\phi} \cos m\phi - b_m(\rho) e^{jm\phi} \sin m\phi] d\rho d\phi$$

Set,

$$\int_0^{\rho} \frac{\mu}{2\pi} \frac{e^{-jkr}}{r} \rho a_m(\rho) d\rho = A_m$$

$$\int_0^{\rho} \frac{\mu}{2\pi} \frac{e^{-jkr}}{r} \rho b_m(\rho) d\rho = B_m$$

So that finally,

$$A_x = \begin{cases} 0 & \text{for } m \neq \pm 1 \\ jA_1 + B_1 & \text{for } m = +1 \\ -jA_{-1} + B_{-1} & \text{for } m = -1 \end{cases} \quad A_y = \begin{cases} 0 & \text{for } m \neq \pm 1 \\ A_1 - jB_1 & \text{for } m = +1 \\ A_{-1} + jB_{-1} & \text{for } m = -1 \end{cases}$$

From these results we can draw the two following conclusions:

(1) Only excitations the characteristic feeding subscript of which is $i=1$ or $i=n-1$ will produce a field on the axis of the antenna.

(2) The field aroused by ${}^n I_1$ and ${}^n I_{n-1}$ on the axis of the antenna will be circularly polarized, where the ${}^n I_1$ feeding excites a field with an opposite sense of polarization than the ${}^n I_{n-1}$ feeding.

These properties were also measured, and it will be seen that the results obtained agree with the conclusions derived here.

III. THE EXPERIMENTAL WORK

In the previous chapter valuable results were derived as to some aspects of the field of the equally spaced, self-complementary, n-arm antenna, but with no reference to a specific shape of the arms. In this chapter the spiral antenna, which is a special case of the above discussed antenna, will be considered, and the results of the experimental investigation upon this antenna will be presented.

Before stating these results, the program of the measurements will be summarized; its connection to the solution of the idealized spiral antenna will be shown, and the measuring apparatus will be briefly described.

A. The Solution for the Field of the Idealized Spiral Antenna

The theoretical solution for the idealized antenna serves as a guide as to what features should be sought and measured in the spiral antenna, which has a small number of arms. This solution also helps to interpret the results of the measurements, and as will be seen later, these results indicate that the fields of the different spiral antennas are closely related, irrespective of the number of arms of the antenna. So before starting to describe the details of the measurements, the theoretical solution will be briefly summarized.

It was found² that the following set of modes

$$\infty F_m(r, \theta, \phi) = e^{jm\phi} \infty C_m(r, \theta) \quad (3.1)$$

would be a solution to the electro-magnetic field of the antenna.

${}^{\infty}F_m$ - is a kind of Herz-Potential.* The superscript indicates that this potential is referred to the spiral antenna which has an infinite number of arms. The subscript m is the mode number.

${}^{\infty}C_m$ - is a complicated function of r and θ , and depends on m .

$e^{jm\phi}$ - refers to the way the antenna is fed. It suggests a feeding in the center of the antenna, which injects a current, constant in amplitude, the phase of which varies continuously from arm to arm (Fig. 7).

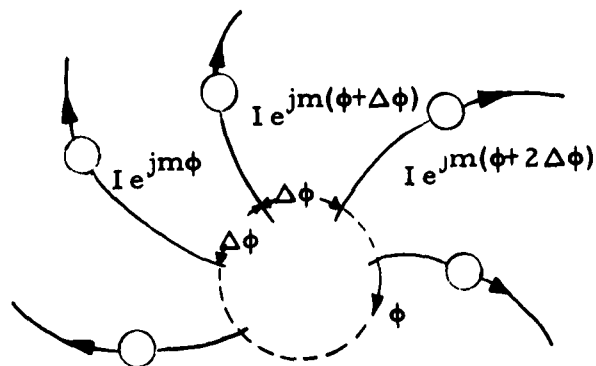


Fig. 7. --The excitation of the idealized spiral antenna

The phase variation of these infinitesimal generators is $2\pi x m$ per revolution. To what extent the different modes will be propagated, will therefore depend upon the way the antenna

* The definition of this Herz-Potential is so that the electric field will be derived from this potential by the following formula:

$$\mathbf{E} = \beta \nabla x \hat{z} {}^{\infty}F_m + \nabla x \nabla x {}^{\infty}F_m$$

Comparing this to the regular Herz-Potential presented in page 10 (see footnote there), it follows that

$${}^nF_{i1} = \beta {}^{\infty}F_m \quad \text{and} \quad {}^nF_{i2} = {}^{\infty}F_m$$

is excited; note that m may be either positive or negative.

The main features of the field of this antenna will be the following:

(1) For any constant r and θ the phase will progress linearly by $m \times 2\pi$ per revolution in ϕ .

(2) The far field will be circularly polarized; the sense of polarization will depend upon m , whether it is positive or negative. In other words, the sense of rotation of the electric vector will depend upon m . Now, of course, m is the same for both sides of the antenna, but the direction of propagation is reversed when crossing the plane of the antenna, so that the fields propagated toward the opposite sides of the antenna will have an opposite sense of polarization. It will be convenient to define a "preferred sense of polarization" as being the polarization of the field when the electric vector is rotating in the same sense as the spiral arms expand. Or describing the preferred polarization with reference to a pair of right and left handed helices, a field with the preferred polarization will be a field with such a polarization that both helix A and B will receive a field which is preferred by them. The sense of the windings of the helices and the sense of the spirals is as indicated in Fig. 8.

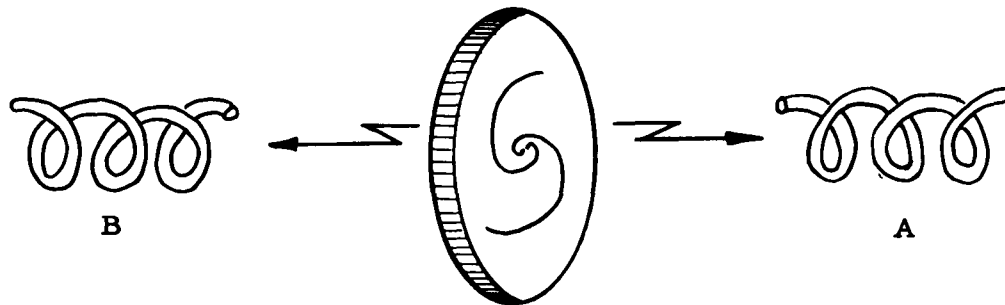


Fig. 8. --The "preferred" sense of polarization

(3) The pattern of the different modes can be seen in reference 2; these patterns were calculated for $a = 1/3$ (1.1), and for $m = 1, 2, 3$. The patterns for m and $-m$ are identical.

(4) Near the plane of the antenna, the fields will decrease very rapidly for increasing r , but the higher m is, the less pronounced will this decrease be.

B. Some Remarks on the Aims of the Measurements

Any spiral antenna can be thought of as being an approximation to the idealized spiral antenna. The program of the measurements has been set up so as to find out how close this approximation actually is. More specifically, an essay has been made to excite the different modes that were indicated by the theoretical solution. The fact that until now modes which have the unpreferred sense of polarization have not yet been found, suggested that an effort should be made, using more elaborate methods of excitation as well as spiral antennas with a higher number of arms, to check this point further.

The more arms the antenna has, the closer it approximates the idealized antenna; also the feeding system can be made to resemble more the $e^{jm\phi}$ excitation.

Note that the characteristic feeding ${}^n I_m$ (2.5), exciting the n -arm antenna, will be the closest approximation to the $e^{jm\phi}$ excitation, but this feeding could as well approximate the $e^{j(m+np)\phi}$ feeding, where p is a positive or negative integer.

This "ambiguity" could serve as a way of illustrating the main result of Chapter I, namely, that the series expansion of the electro-magnetic field will include only terms for which $m = i + pn$ (see 2.11-2.13).

Of special interest was to find out how would the antenna respond to the ${}^n I_{n-1}$ characteristic feeding, which is an

approximation to the $e^{j(n-1)\phi}$ feeding (and also to all other feedings for which $m = -1 + pn$).

C. The Measuring Apparatus

1. Introduction

The measurements were carried out on 2, 4, and 6-arm antennas, excited by many different feeding arrangements. The measured features were the pattern of the field strength, the polarization of the far field and the phase variation of the field. The spiral antennas of which the field was measured were made by photo-engraving copper-clad fiber-glass sheets. The diameter of the feeding zone was not more than 10 mm. The arms of the antenna were always self-complementary planes. The operating frequency was 3000 Mc/s. All measurements were performed in an anechoic chamber, where the reflection of the walls was less than -20 db.

A description of the different antennas measured, and their feeding arrangements, will be given under the sections dealing with each specific antenna.

For a summary of the results of the measurements see Figure 37.

2. The phase variation measurements

The arrangement for the phase variation measurements is shown in Fig. 9. A signal was fed into the antenna and detected by a very small coaxial probe which could move along a radius of the antenna. The signal received by the probe, when the antenna was turned around its axis, was introduced into one arm of a Magic T. To the opposite arm of the Magic T a signal from the same transmitter was introduced through a moving probe inserted in a slotted wave-guide. The sum of these two signals was amplified and detected. The probe in the wave-guide was placed so as to cancel the signal from the antenna. Note that the probe has two degrees of freedom: the depth of penetration, which governs the amplitude; and the

movement along the wave-guide, which changes the phase.

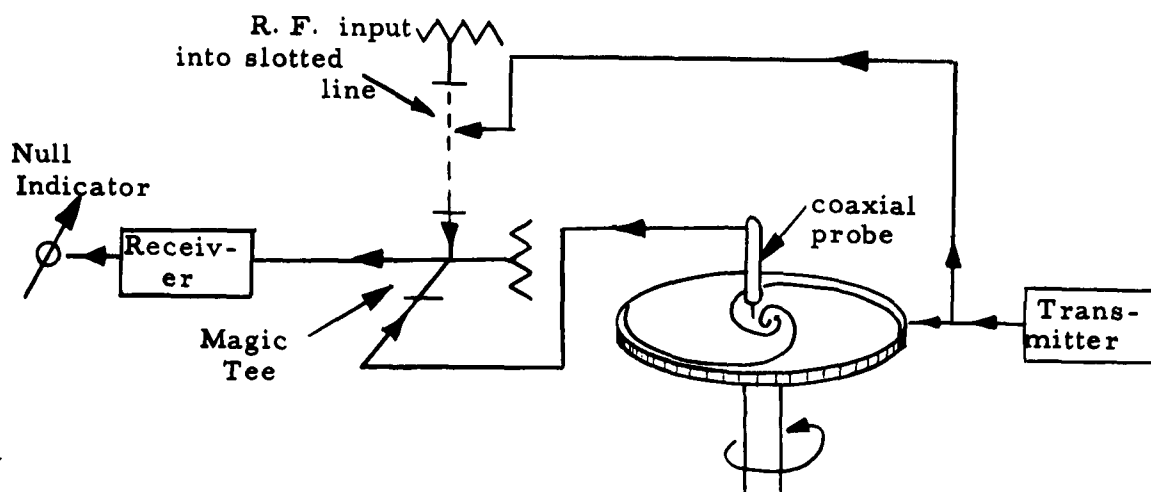


Fig. 9. -- The arrangement for the phase measurements

Now when the antenna is rotated, also the probe is moved, so that both signals cancel. The successive positions of the probe show the phase variation of the field of the antenna.

The phase progression will be called positive if it increases when the antenna is turned in the direction indicated in Fig. 9.

The phase measurements were performed in three distinct regions (Fig. 10):

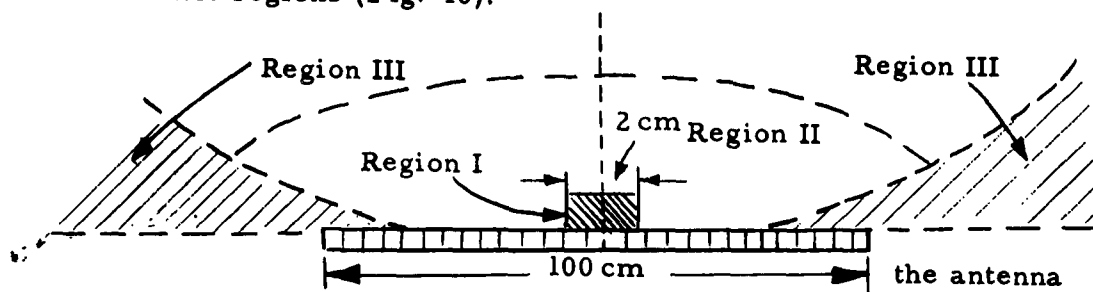


Fig. 10. -- The different regions

Region I .: very near to the plane of the antenna and close to its axis (less than 2 cm off the axis).

Region II : the main region.

Region III: very near to the plane of the antenna, but far away from the axis.

Phase measurements have the advantage that we always have a phase variation of $2\pi \cdot m$ where m is an integer, when turning once around the antenna. This, of course, does not mean that the only term of the Fourier series present is the $e^{jm\phi}$ term. It only means that the main term of the series is $e^{jm\phi}$, and from the linearity of the phase variation we can estimate the importance of the other terms.

3. Pattern measurements

The pattern was measured in a plane perpendicular to the plane of the antenna, through its axis. The spiral antenna was used as transmitting antenna, whereas the field was received by a horn or a helix, as is indicated in the different figures. All measurements were calibrated by an attenuator.

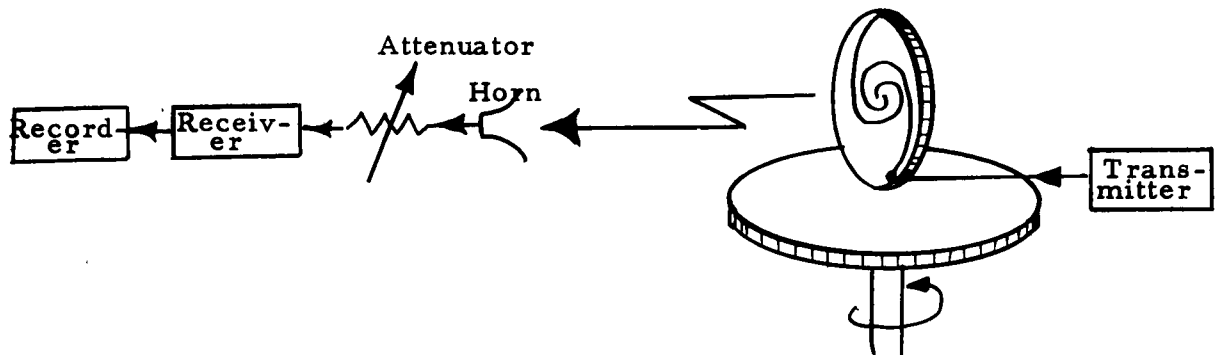


Fig. 11. --Arrangement for pattern measurements

4. Polarization measurements

When pattern measurements are performed with a helix, then the ratio of the two fields, received from the two opposite sides of the antenna, gives us a measure of the two opposite circularly polarized components of which the radiated field is composed. The polarization is also measured by interchanging two helices of opposite senses.

D. Results of Measurements on the 2-Arm Spiral Antenna - 2A

1. The feeding arrangement

The feeding arrangement of the 2A-antenna (Figs. 12, 13) consists of a coaxial line, the inner conductor of which is connected to one of the arms, whereas the outer conductor is connected to the second arm. The feeding resulting from this arrangement is the 2I_1 characteristic feeding (see II, B).

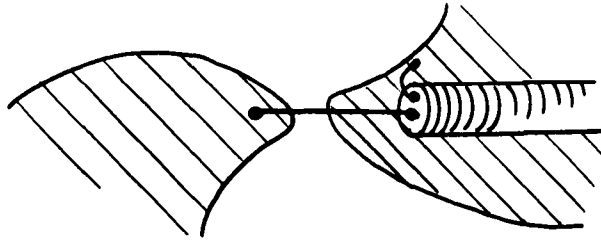


Fig. 12. --The feeding arrangement of the 2A-antenna

2. The phase variation

Region I : The field was found to have a gradual phase variation of $+2\pi$, when turning once around the antenna (see Fig. 19). The phase variation was always positive (see Ch. III, C, 2).

Region II: same as for region I.

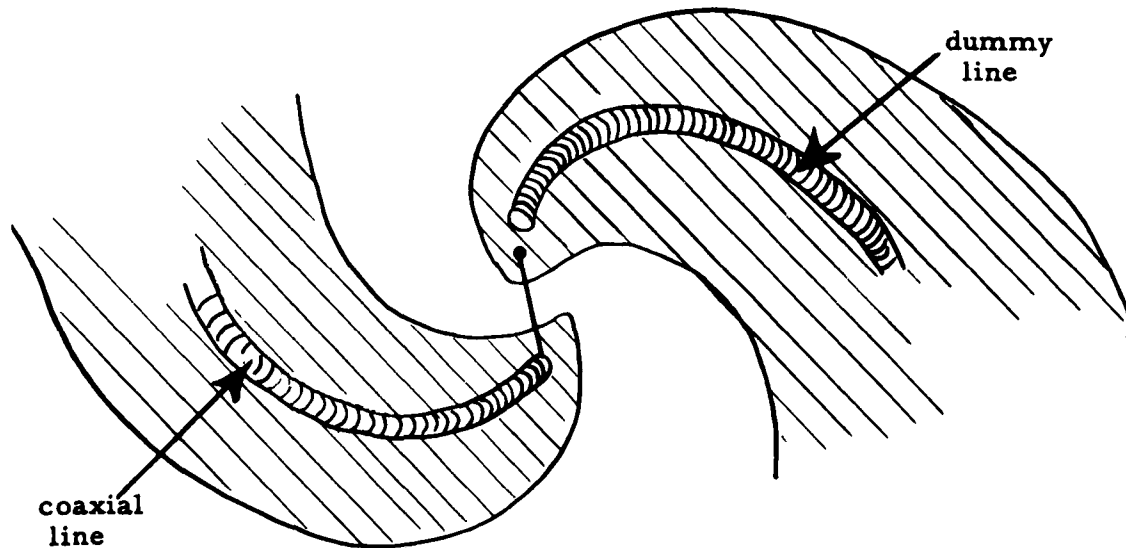


Fig. 13. --The feeding line coming along the arm

3. The pattern

The pattern had maximum field intensity on the axis, and decreased symmetrically in both directions (see Figs. 20 and 21).

4. The polarization

The polarization was found to have always the preferred sense.

E. Results of the Measurements on the 4-Arm Spiral Antenna-4A

1. The feeding arrangement

The feeding arrangement of the 4A-antenna consists of a coaxial line, the inner conductor of which is connected to two opposite arms, while the outer conductor is connected to the two remaining arms. This feeding arrangement gives rise to input currents of the $I_1 I_2$ type.

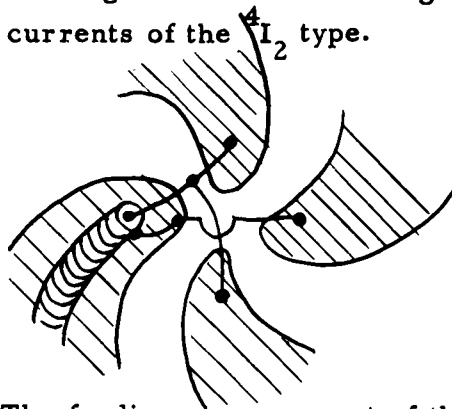


Fig. 14. --The feeding arrangement of the 4A-antenna

2. The phase variation

Region I : The phase progression was found to be $+2 \cdot 2\pi$ when turning once around the antenna, being always positive.

Region II : Same as region I (see Fig. 22).

Region III: Even though the data obtained by this measurement were not very clear, as the field in this region was very weak, it seems to be safe enough to say that the phase variation was $2\pi \cdot 6 (!)$, and always positive (Fig. 22).

3. The pattern

The pattern had a null on the axis of the antenna (see Fig. 23).

4. The polarization

The polarization of the field was in the preferred sense (see Fig. 24). A difference of at least 10 db was found between the reception of two helices of opposite senses.

F. Results of the Measurements of the 4-Arm Spiral Antenna-4B

1. The feeding arrangement

Two coaxial lines feed the two pairs of opposite arms of the 4B-antenna (see Fig. 15). The two lines can be fed independently, i. e., their respective phase and amplitude can be varied. This feeding arrangement gives rise to many different feeding vectors, among them the characteristic feedings 4I_1 and 4I_3 . These two are the only ones that were considered here.

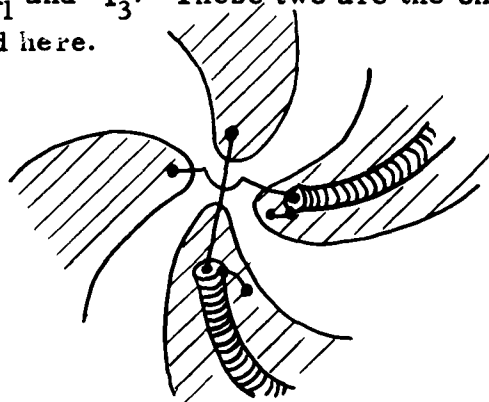


Fig. 15. --The feeding arrangement of the 4B-antenna

4I_1 will be excited when the outputs of the two lines have the same amplitudes and a phase difference of 90° . If the phase of one of the lines will be reversed, we shall get the 4I_3 characteristic feeding.

Actually, the phase and the amplitude of the output of the two lines were adjusted in the following way: in order to get a 4I_3 feeding, the phase and the amplitude

were adjusted so as to get a minimum of field on the axis of the antenna, whereas to get the 4I_1 feeding, the phase and the amplitude were adjusted to give a maximum. The justification of this procedure will become apparent from the results of the phase variation in region I.

2. The phase variation

For 4I_1 , region I : The phase varied with $+2\pi$, when turning once around the antenna.

Region II: Same as region I.

For 4I_3 , region I : The phase had a variation of -2π (!)

Region II: The phase variation was $+6\pi$.

For all these results see Fig. 25.

3. The pattern

The pattern was actually adjusted to have a maximum for the 4I_1 feeding, and a minimum for the 4I_3 feeding on the axis (see Figs. 26 and 27).

4. The polarization

The polarization was found to be of the preferred sense for both feedings, except for the field on the axis of the antenna, when fed with the 4I_3 feeding. In this case, both circular polarizations were present in about an equal amount. Note that the field on the axis was very weak, but nevertheless the presence of both polarizations could not be attributed to random signals, as the preferred polarization had a distinct minimum; whereas the opposite polarization had a maximum for both small variations of the phase of the feeding currents, as well as small deviations from the axis of the antenna.

G. Results of the Measurements on the 4-Arm Spiral Antenna-4C

1. The feeding arrangement

In the 4C-antenna the inner conductor of the coaxial line is connected to one arm, the outer conductor is connected to the opposite arm and the two remaining arms are left unconnected. As shown in II, C, 2, this feeding contains an equal amount of the two characteristic feedings 4I_1 and 4I_3 .

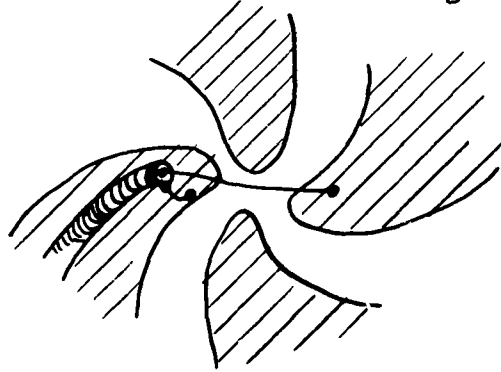


Fig. 16. -- The feeding arrangement of the 4C-antenna

2. The phase variation

Region I : The phase was found to progress by $+2\pi$ when turning once around the antenna (see Fig. 28).

Region II: In the inner part of region II the phase variation was $+2\pi$. For the outer part the phase variation was $+6\pi$, and in the border between these two parts the phase variation was a mixture of both 2π and 6π , (see Fig. 28).

3. The pattern

The pattern had a maximum on the axis, but also two side lobes (see Fig. 29).

4. The polarization

The polarization had the preferred sense (see Fig. 30).

H. Results of the Measurements on the 6-Arm Spiral Antenna-6A

1. The feeding arrangement

In the 6A-antenna the outer conductor of a coaxial line is connected to three arms, spaced 120° apart; while the inner conductor is connected to the three remaining arms. The feeding currents are of the 6I_3 type (see II, C, 4).

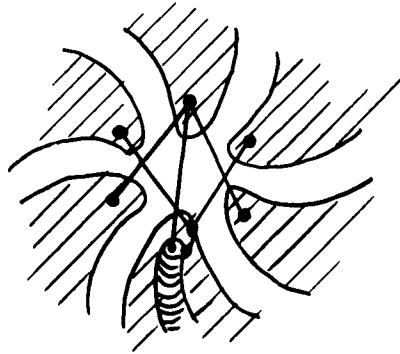


Fig. 17. --The feeding arrangement of the 6A-antenna

2. The phase variation

Region I : The phase variation was 6π .

Region II : The phase variation was 6π (see Fig. 31).

Region III: The phase variation was 18π (see Fig. 31).

3. The pattern

The pattern had a null on the axis of the antenna (Fig. 32).

4. The polarization

The field had a polarization of the preferred sense. Actually, there was a difference of about 10 db between the preferred and the opposite polarization (see Fig. 33).

I. Results of the Measurements on the 6-Arm Spiral Antenna-6B

1. The feeding arrangement

The outer conductor of a coaxial line is connected to two adjacent arms of the 6B-antenna, while the inner conductor is connected to the two opposite arms. The two in-between arms are left unconnected. This feeding arrangement

gives rise to currents, which are a combination of the 6I_1 and 6I_5 characteristic feedings (see II, C, 3).

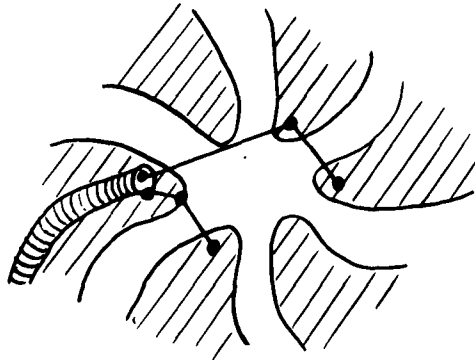


Fig. 18. --The feeding arrangement of the 6B-antenna

2. The phase variation

Region I : The phase variation was $+2\pi$ (see Fig. 34).

Region II: In the inner part of region II the field had a phase variation of $+2\pi$, whereas in the outer part the phase variation was $+10\pi$ (Fig. 34). In the border between the inner and the outer part the phase variation was a combination of 2π and 10π (see Fig. 35).

3. The pattern

The pattern had a null on the axis as well as two side lobes (see Fig. 36).

4. The polarization

The polarization of the field had the preferred sense.

J. Conclusion

This section included only experimental results without any interpretation. The interpretation has been left for the next chapter so as not to mix the actual data with any assumptions.

To make the comparison of the different results easier, all the measurements are summed up in Fig. 37.

IV. CONCLUSIONS

A. A Summarized Presentation of the Conclusions

The object of this chapter is to show how the information obtained from the measurements, together with the theoretical considerations developed in Chapter I, can give us a fairly accurate estimation of the electro-magnetic field of an n-arm spiral antenna, which has any kind of feeding arrangement.

The arguments presented in this chapter will proceed along the following line: first it will be shown that the field of an n-arm antenna, when fed by one of its characteristic feedings ${}^n I_1$, will be approximately equal to the field of the i-th mode of the idealized antenna. This means that the main properties of the idealized antenna are preserved in the spiral antenna, even if it has only a small number of arms.

Next, some corrections will be introduced in the field of the idealized antenna, so as to get a still better approximation in the case of a small number of arms.

Finally, as any feeding arrangement can be decomposed into the basic characteristic feedings, and as the field aroused by each of the characteristic feedings is approximately known; then, by applying the principle of superposition, the total field can be estimated.

B. A Detailed Presentation of the Conclusions

The first step will be to compare the results of the measurements obtained for antennas, which have different numbers of arms, but are all fed by a characteristic feeding which corresponds to a certain mode of the idealized antenna. Or, in other words, to compare fields which may have any superscript, but have all the same subscript.

Considering the 2F_1 field (see Chapter III, d and Figs. 19-21), we can see that it is very similar to 4F_1 (see Chapter III, F and Figs. 25, 26), and moreover, both have similar features to ${}^\infty F_1$, regarding the pattern, the phase and the polarization of the field (see III, A and reference 2).

Next, a consideration of 4F_2 (see III, E and Figs. 22-24) will show that this field is similar to F_2 .

Furthermore, the main fields (i. e., the fields in region II), having an $i=3$ as 4F_3 (see III, F and Figs. 25, 27) and 6F_3 (see III, H and Figs. 31-33), are similar to the ${}^\infty F_3$ field. Note also that the angle between the two side lobes in the $i=3$ case is somewhat bigger than for the $i=2$ case, a fact which is indicated also by the calculations for the idealized spiral antenna.

These examples show that it would be plausible to assume that

$${}^n F_i \text{ has approximately the same form as } {}^\infty F_i \quad (4.1)$$

for

$$1 \leq i \leq n-1$$

For example, this statement indicates that the 6F_5 field, which is the field excited by the 6I_5 characteristic feedings, namely by

$${}^6I_5 = [1, e^{j300^\circ}, e^{j240^\circ}, e^{j180^\circ}, e^{j120^\circ}, e^{j60^\circ}]$$

is similar to the field of the idealized antenna, when fed by a feeding with a ϕ dependence as $e^{jm\phi}$, with $m=5$; although, intuitively, it would seem that this 6F_5 field should be similar to the $m=-1$ mode. This example shows that the spiral antenna has a preference of the so-called "preferred sense of polarization." Note that the "preferred sense of polarization" depends upon the sense in which the spirals of the antenna are wound.

Now some correction terms will be introduced, and these terms will point out the small differences which exist among the fields which have the same subscript. These terms

depend on the superscript, i. e., upon the number of arms.

A more careful examination, especially in the regions I and III, shows that there is some deviation from the above-mentioned assumption (4.1). Particularly, phase measurements on the axis of the antenna show that 4F_3 includes also a field which seems to be of the ${}^\infty F_{-1}$ type. Its amplitude is so weak that it can only be detected on or near the axis, where the main field ${}^\infty F_3$ has a null.

The measurements in region III of the 4A-antenna also show that in addition to ${}^\infty F_2$, there exists a field with a phase variation of 12π per revolution. This field can be thought of as a weak ${}^\infty F_6$ field. This field can only be detected in region III, where the main field is already very weak; but ${}^\infty F_6$, which is attenuated less with increasing radius, has still a considerable amplitude. In fact, ${}^\infty F_6$ will be the main field in region III.

The same can be said about the ${}^\infty F_9$ field which can be measured in region III of the 6A-antenna.

A ready explanation why, of all the modes that exist, the $m = -1$ in 4F_3 , $m = 6$ in 4F_2 , and $m = 9$ in 6F_3 should appear, was already given by formula (2.11) subject to the restriction given in (2.13).

Namely:

$${}^n F_i = \sum_{m=-\infty}^{\infty} {}^n C_m(r, \theta) e^{jm\phi} \quad m = i + np \quad p = 0; \pm 1; \pm 2, \dots$$

Now if we assume that ${}^n C_m(r, \theta)$ has approximately the same form as ${}^\infty C_m(r, \theta)$ (in 3.1), an assumption which is a complement to the statement (3.1), we may write,

$${}^n F_i \approx \sum_{m=-\infty}^{\infty} a_m {}^\infty C_m(r, \theta) e^{jm\phi} \quad m = i + np \quad (4.2)$$

where a_m is a coefficient which determines the relative importance of the different terms.

(4. 2) actually means that the n-arm antenna will generate a field nF_i which is composed of all the modes of the idealized spiral antenna, for which $m=i+np$, with different amplitudes.

Note that (4. 2) reduces to (3.1) as n tends to infinity.

Now the first higher order mode will be according to (4. 2) $m=i+n$, which is for 4F_2 - $m=6$, and for 6F_3 is $m=9$, as actually measured. Modes of still higher order could not be detected, as fields are so weak at large radii along the plane of the antenna that they are shaded by the background noise (reflections, etc.).

As to the relative amplitudes of the a_m , two facts can be pointed out:

(a) a_i is by far the largest factor; this means that in region II, which is the main region, ${}^\infty F_i$ will practically be the only field of any importance.

(b) a_m for $m<0$ will always be very small.

The discussion so far in this section has been concerned only with antennas fed by characteristic feedings. An examination of the results of the measurements for the 4C-antenna (see III, G and Figs. 28-30), show very clearly that the field is a superposition of the 4F_1 and 4F_3 fields, as predicted by the consideration of II, C 2.

The results of the 6B-antenna (see III, I and Figs. 34-36), agree also very well with the predictions of II, C, 3; i. e., that the field is a superposition of the 6F_1 and 6F_5 fields.

Note also that the angle between the two side lobes is still bigger than for $i=2$ or $i=3$, as the side lobes are a part of the F_5 field.

These two examples demonstrate the validity of the

conclusions of Chapter II concerning the decomposition of any feeding into its characteristic feedings. Likewise, it illustrates the usefulness of this method.

C. Conclusion

To conclude this work the two main results obtained are summed up. First, it has been shown how the field of an n-arm equally spaced self-complementary antenna with arms of any shape and fed by any feeding arrangement, can be decomposed to a set of basic fields. Second, by applying the first result together with experimental data, it has been shown how the field of the equiangular plane spiral antenna, having any number of arms and any type of feeding arrangement, can be estimated,

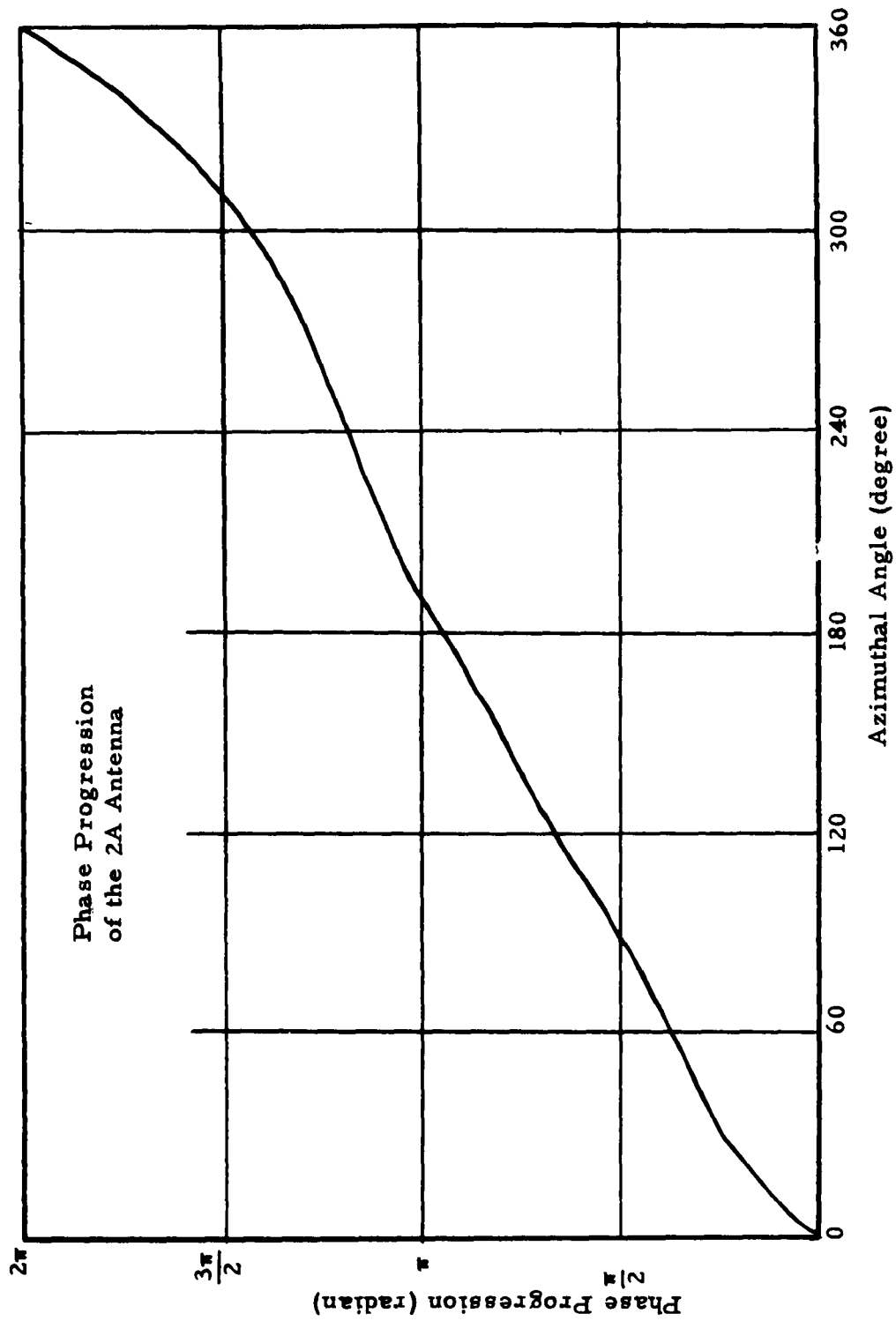


Fig. 19. -- The phase progression of the 2A-Antenna as a function of the azimuthal angle, (see Ch. III, D), as measured in region II, (see Fig. 10).

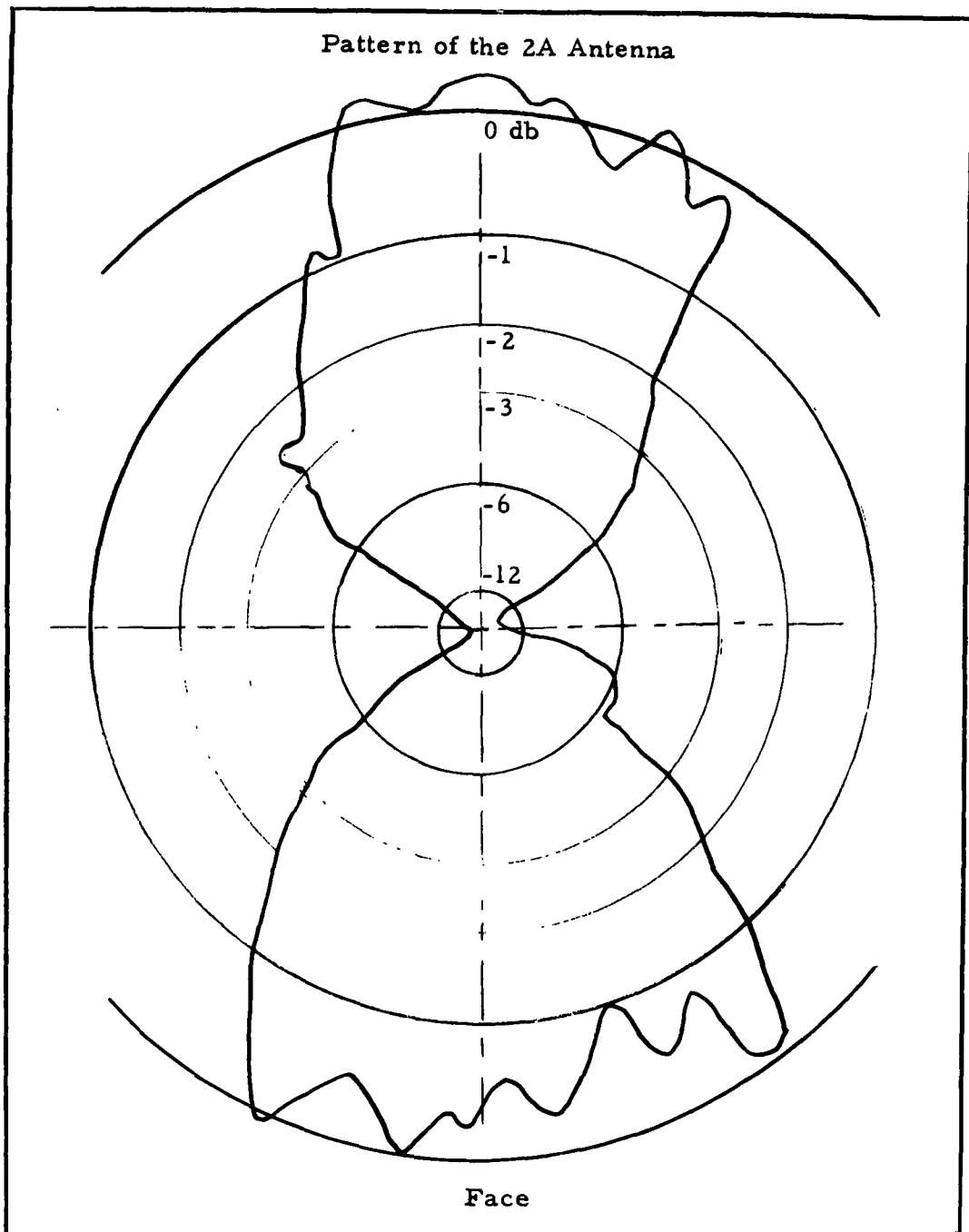


Fig. 20. --The pattern of the 2A-Antenna as measured in a plane perpendicular to the plane of the antenna through its axis, with a horn serving as receiving antenna.

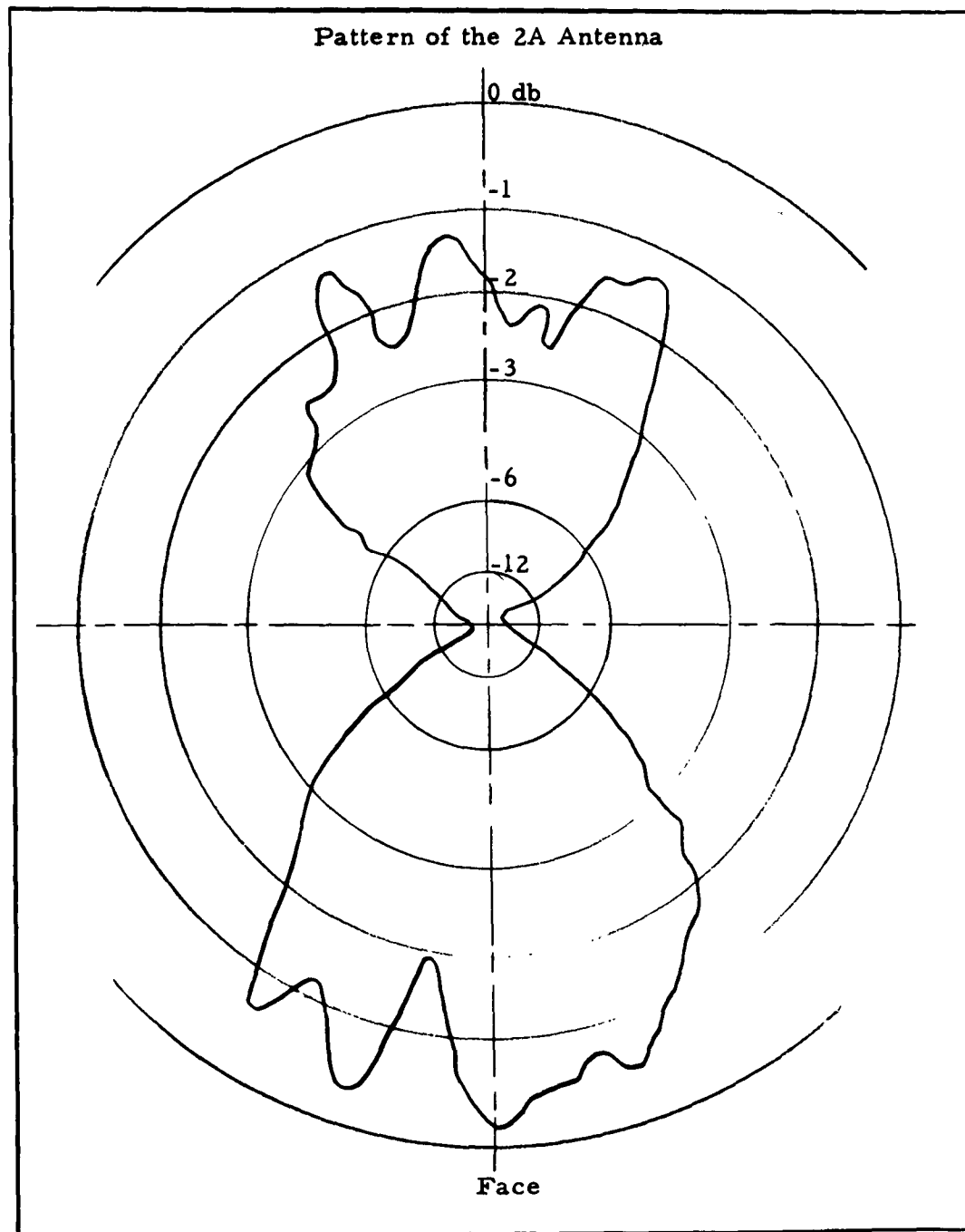


Fig. 21. -- The pattern of the 2A-Antenna as measured in a plane perpendicular to the plane of the antenna through its axis, with a horn serving as receiving antenna.

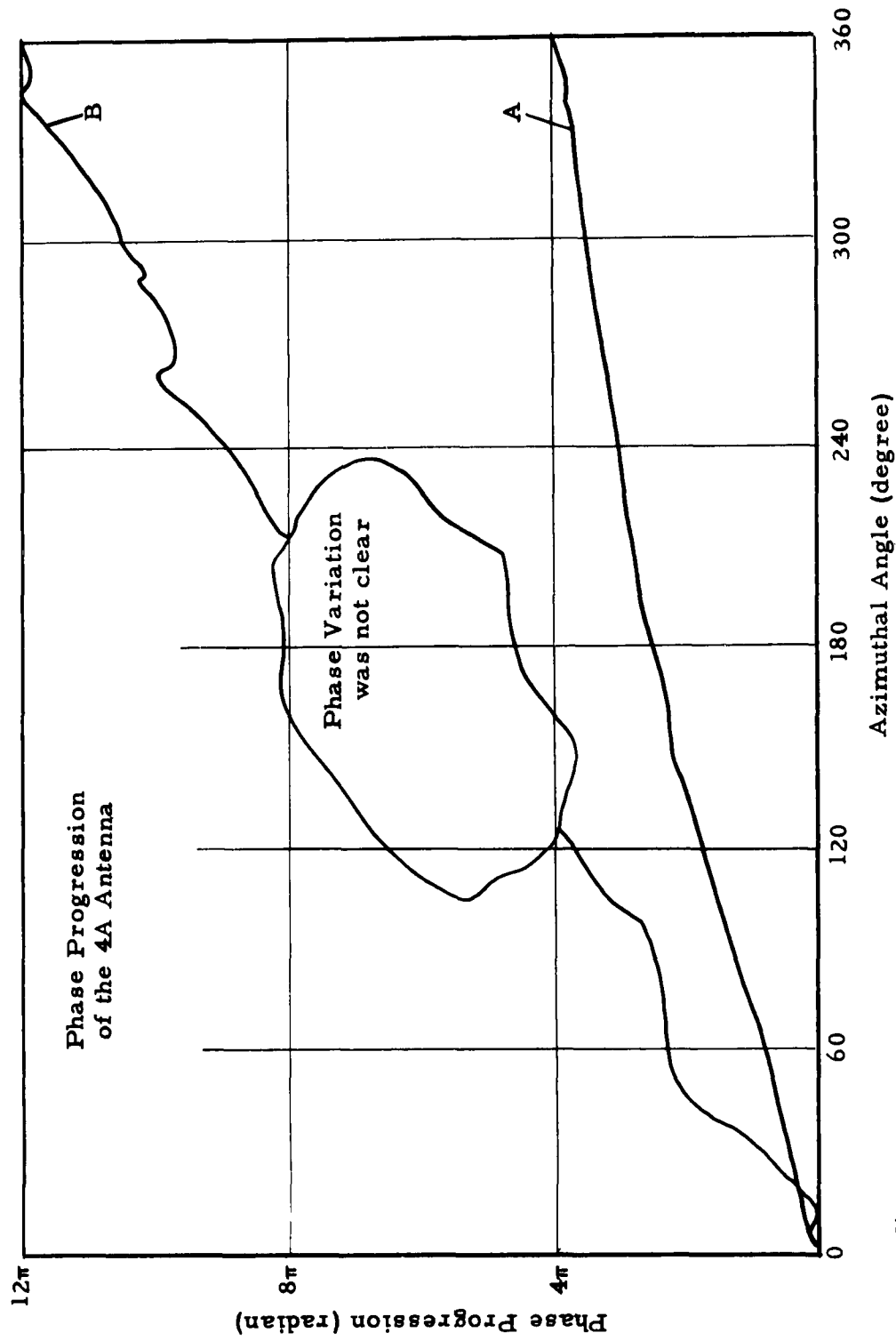


Fig. 22. -- The phase progression of the 4A-Antenna as a function of the azimuthal angle, (see Ch. III, E).
 Curve A: measurements taken in region II. Curve B: measurements taken in region III.

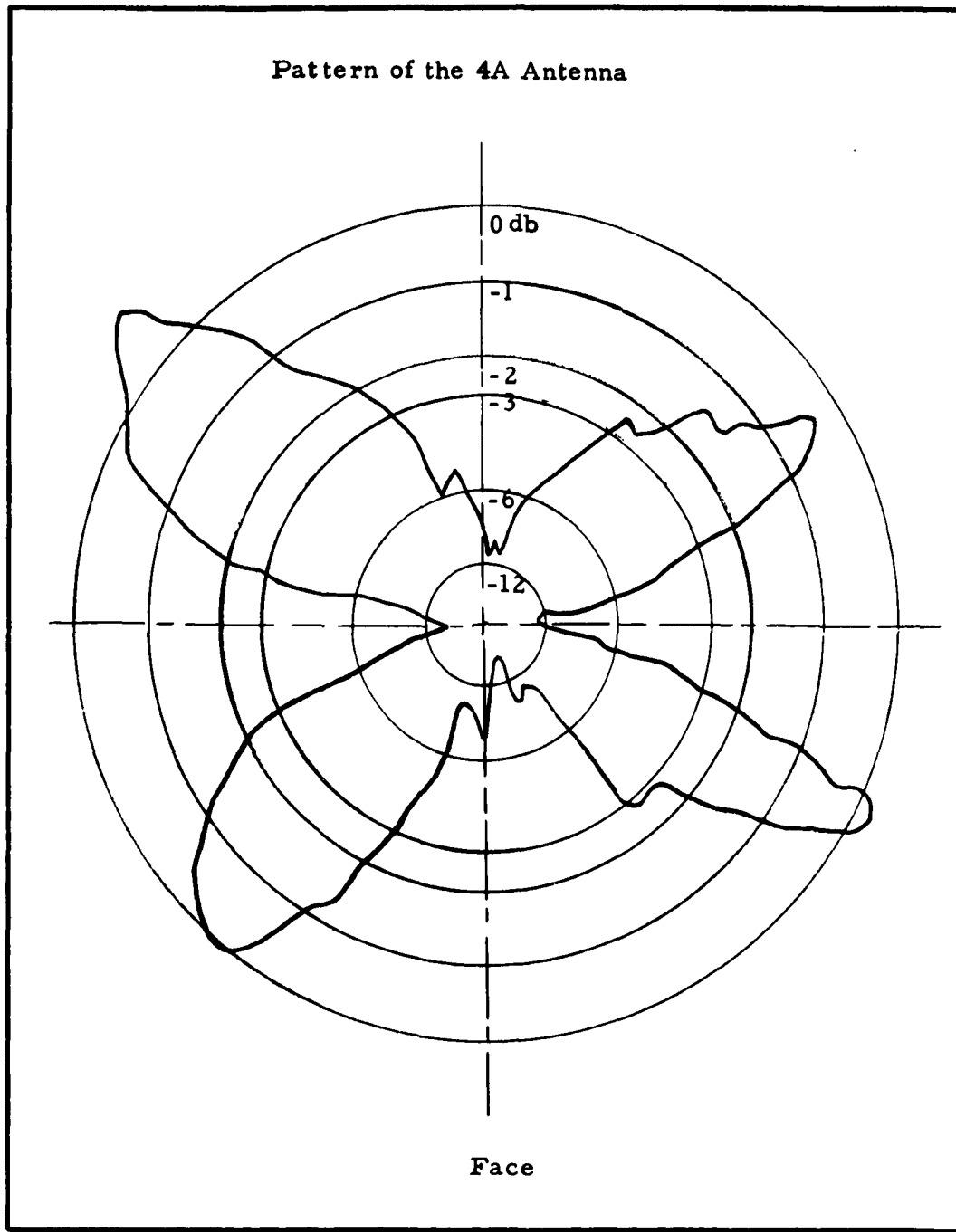


Fig. 23. -- The pattern of the 4A-Antenna as measured in a plane perpendicular to the plane of the antenna through its axis, with a horn serving as receiving antenna.

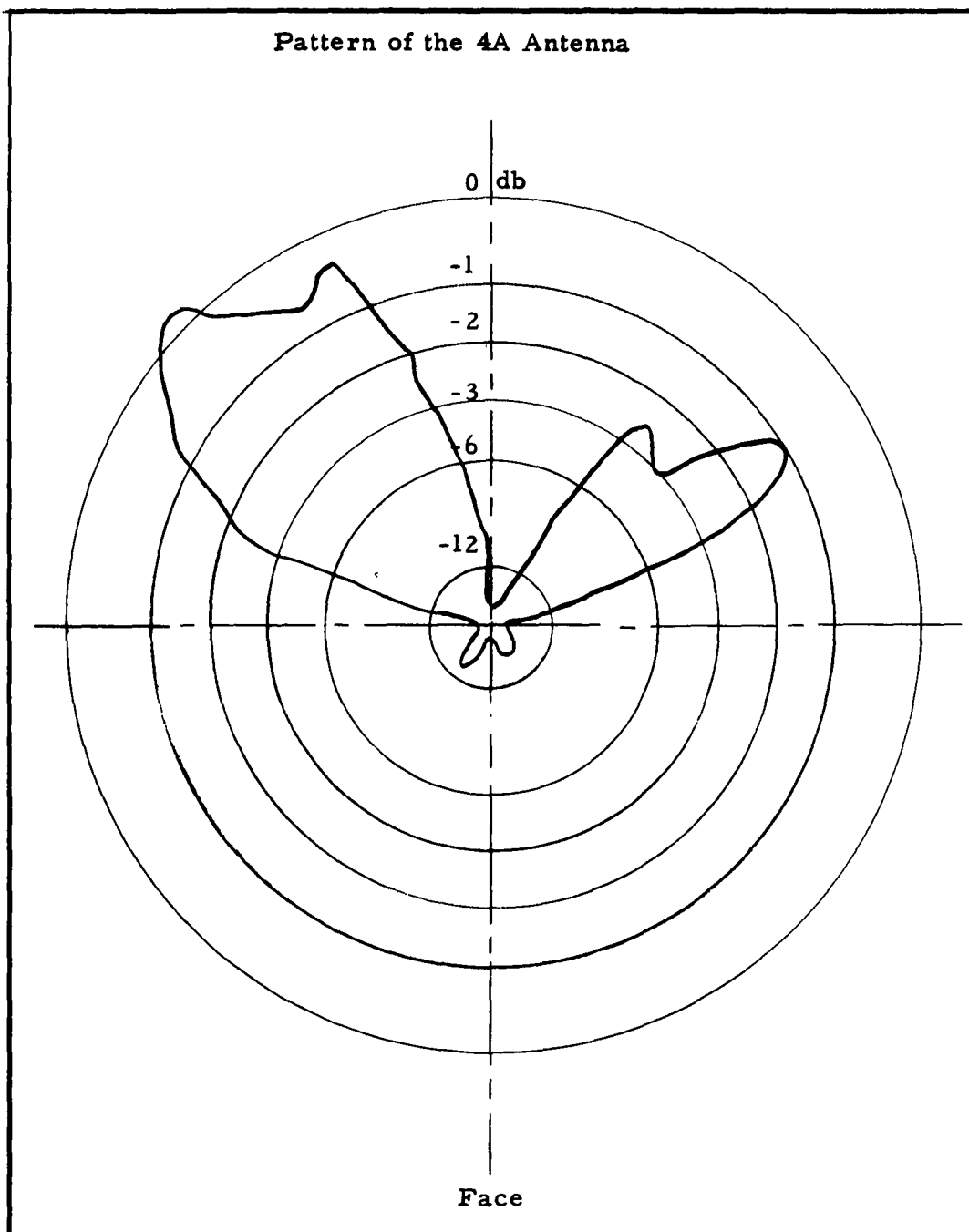


Fig. 24. --The pattern of the 4A-Antenna as measured in a plane perpendicular to the plane of the antenna through its axis, with a helix serving as receiving antenna.

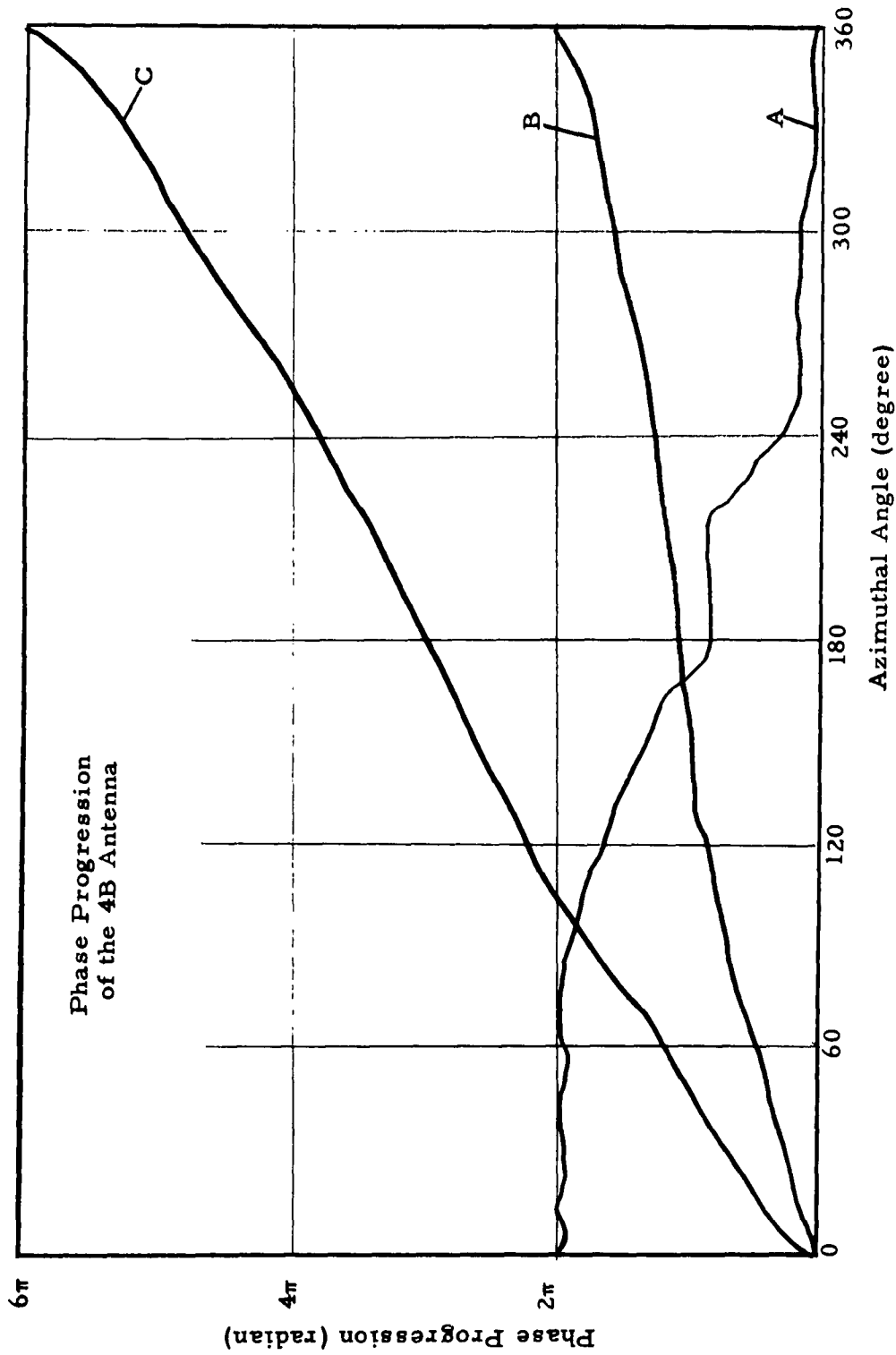


Fig. 25. -- The phase progression of the 4B-Antenna as a function of the azimuthal angle, (see Ch. III, F).
 Curve A: the antenna is fed by the 4I_3 characteristic feeding and measured in region I.
 Curve B: the antenna is fed by the 4I_1 characteristic feeding and measured in region II.
 Curve C: the antenna is fed by the 4I_3 characteristic feeding and measured in region II.

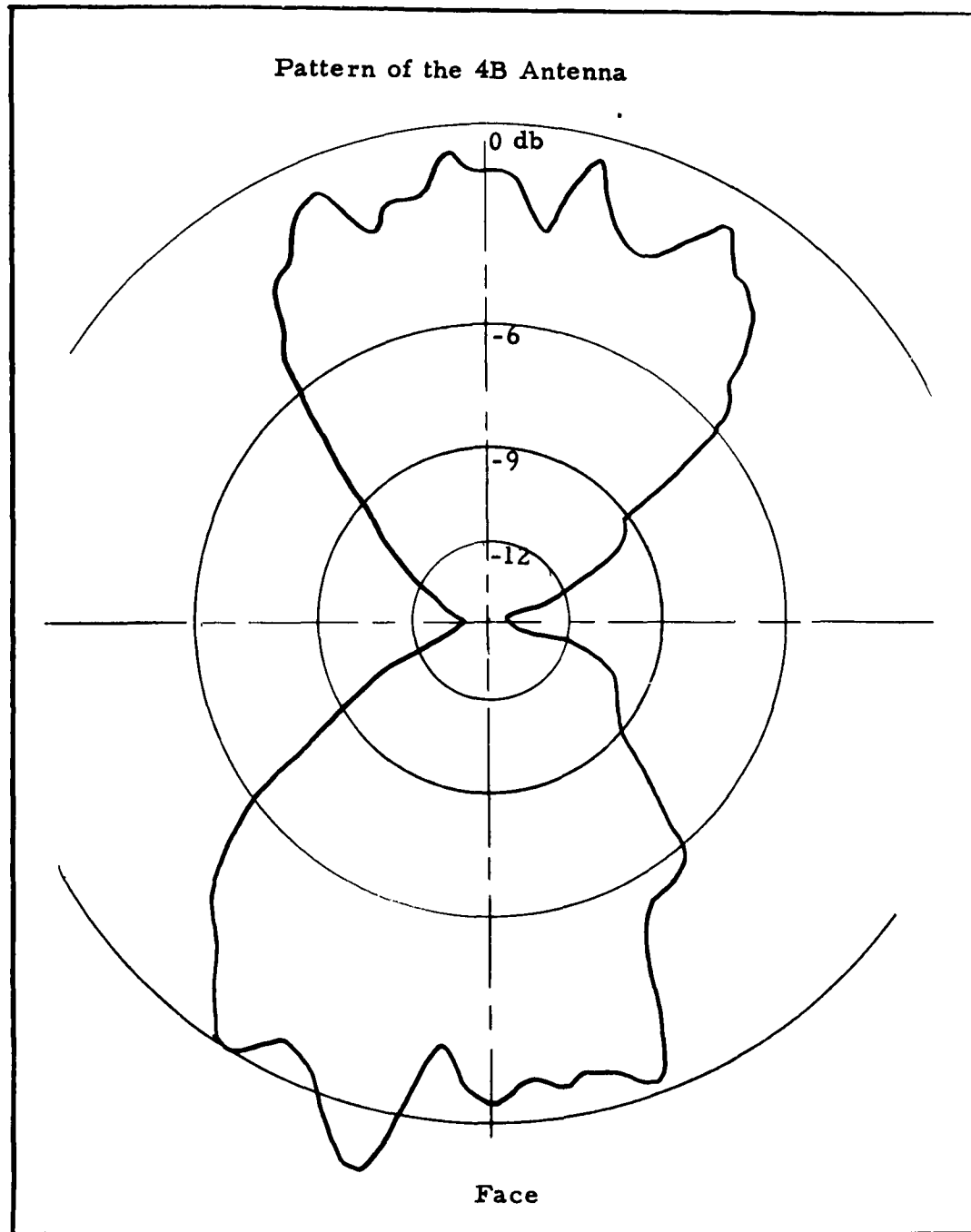


Fig. 26. --The pattern of the 4B-Antenna as measured in a plane perpendicular to the plane of the antenna through its axis, when the antenna is fed by the 4I_1 characteristic feeding. A horn served as receiving antenna.

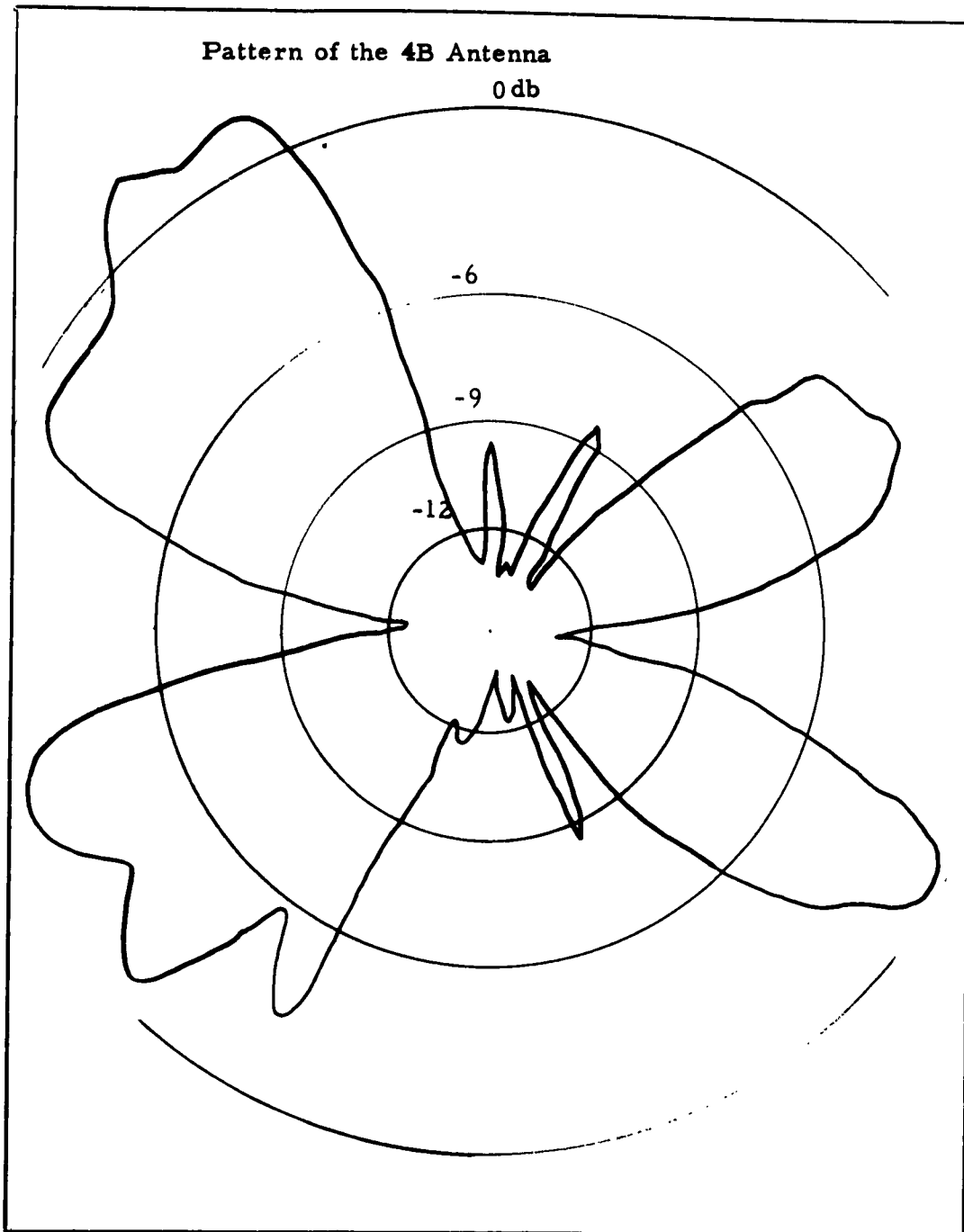


Fig. 27. --The pattern of the 4B-Antenna as measured in a plane perpendicular to the plane of the antenna through its axis, when the antenna is fed by the 4I_3 characteristic feeding. A horn served as receiving antenna.

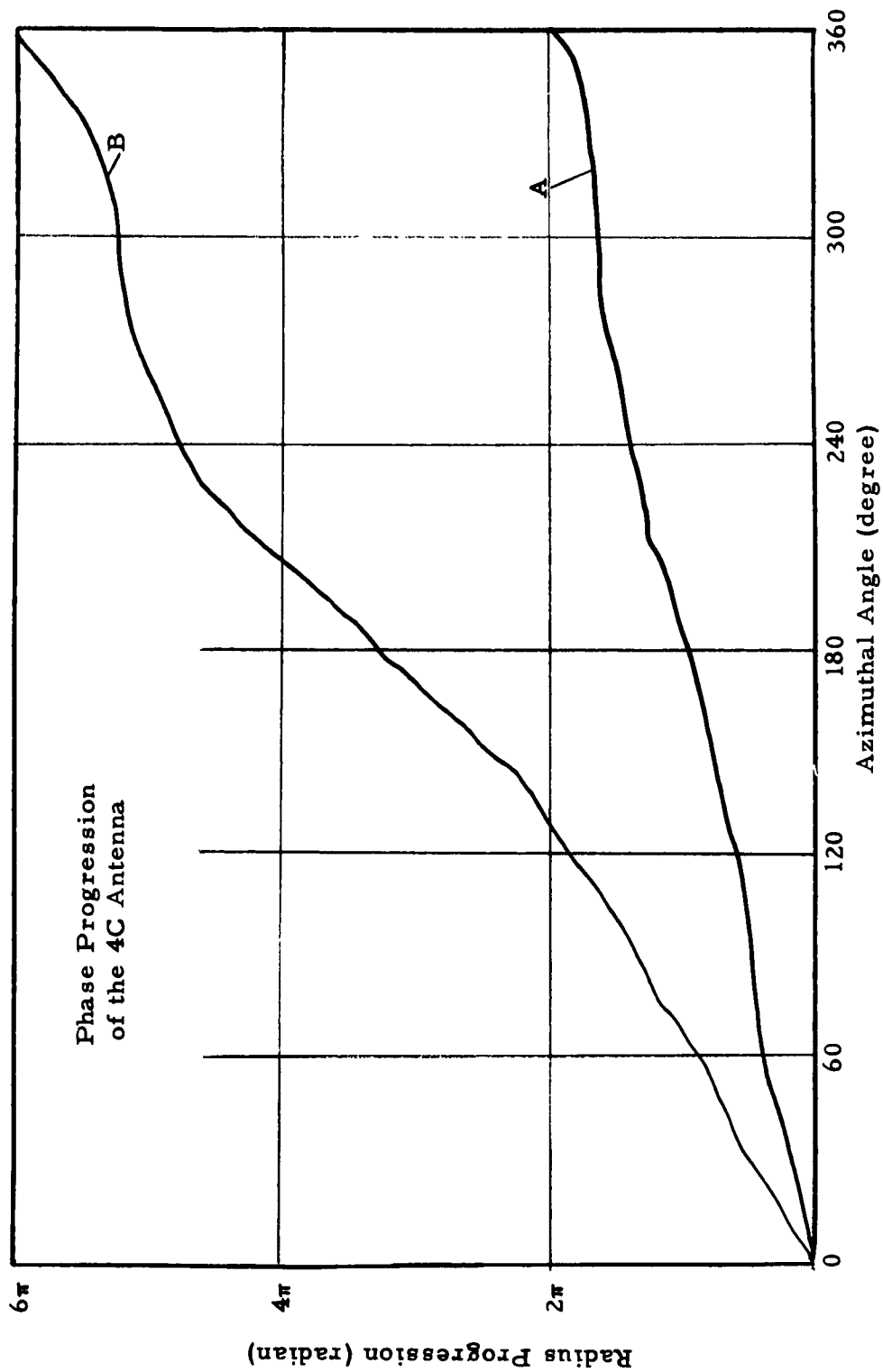


Fig. 28. -- The phase progression of the 4C-Antenna as a function of the azimuthal angle, (see Ch. III, G).
 Curve A: measured in the inner part of region II, (less than 3 cm off the axis).
 Curve B: measured in the outer part of region II, (more than 3 cm off the axis).

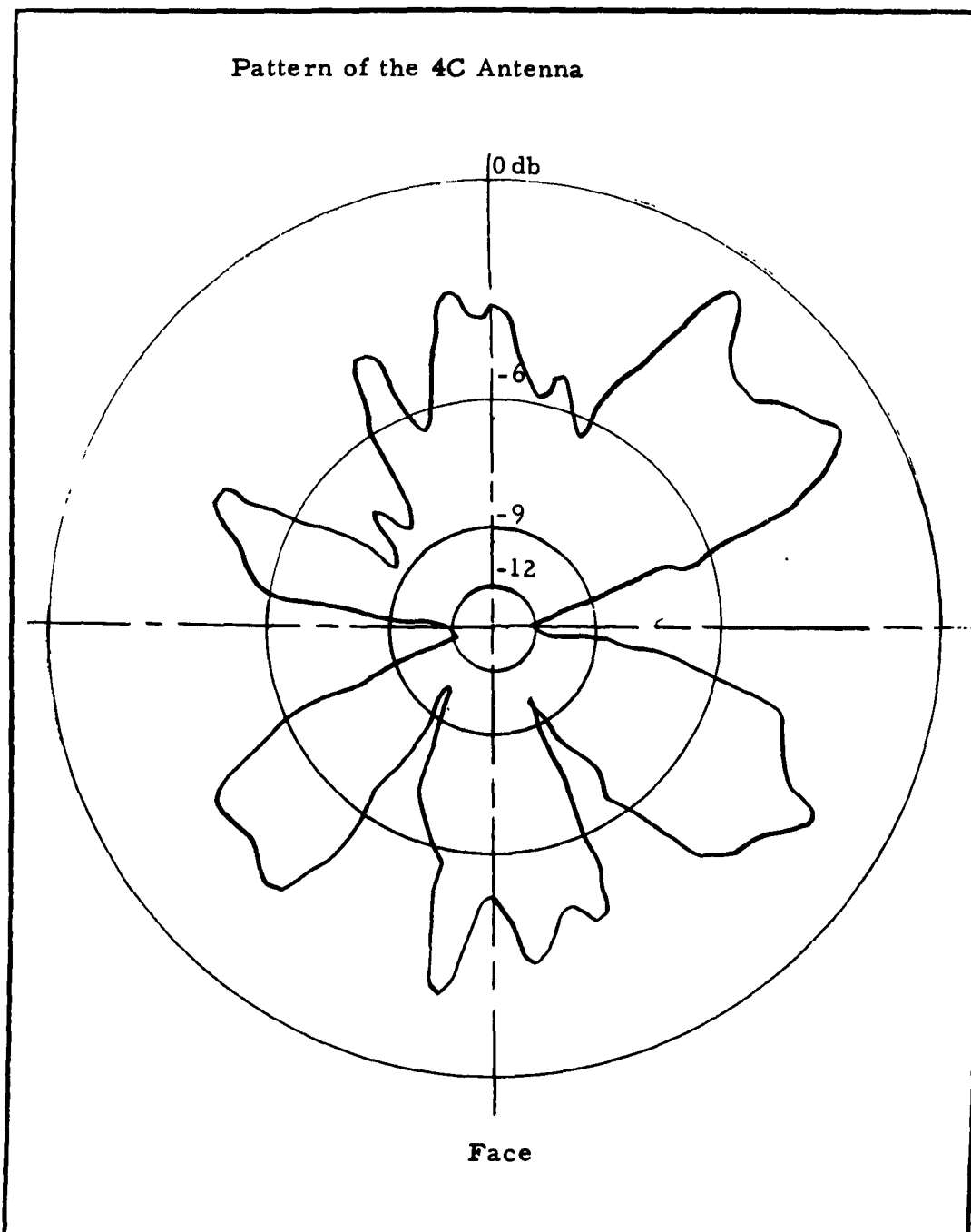


Fig. 29. --The pattern of the 4C-Antenna as measured in a plane perpendicular to the plane of the antenna through its axis, with a horn serving as receiving antenna.

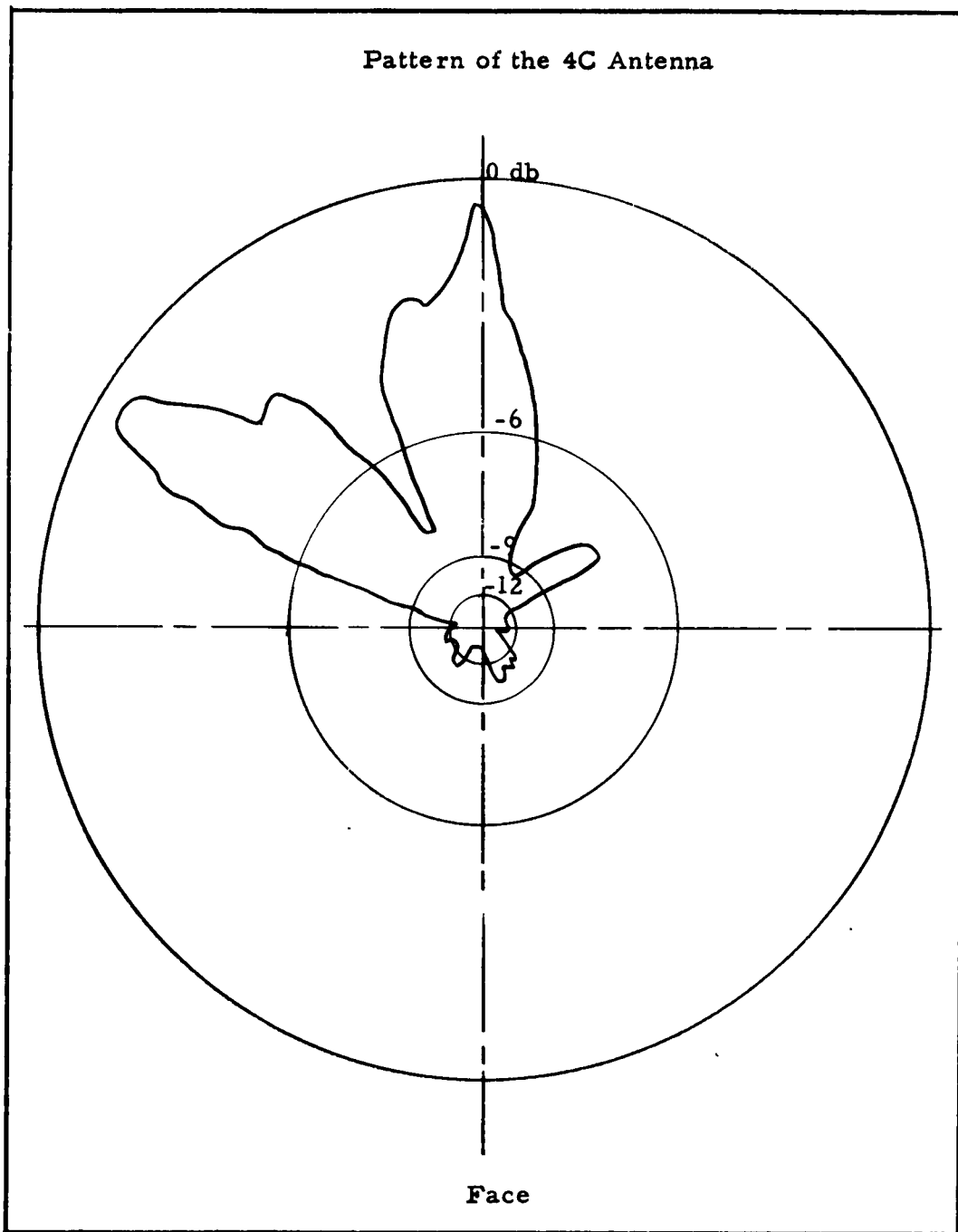


Fig. 30. --The pattern of the 4C-Antenna as measured in a plane perpendicular to the plane of the antenna through its axis, with a helix serving as receiving antenna.

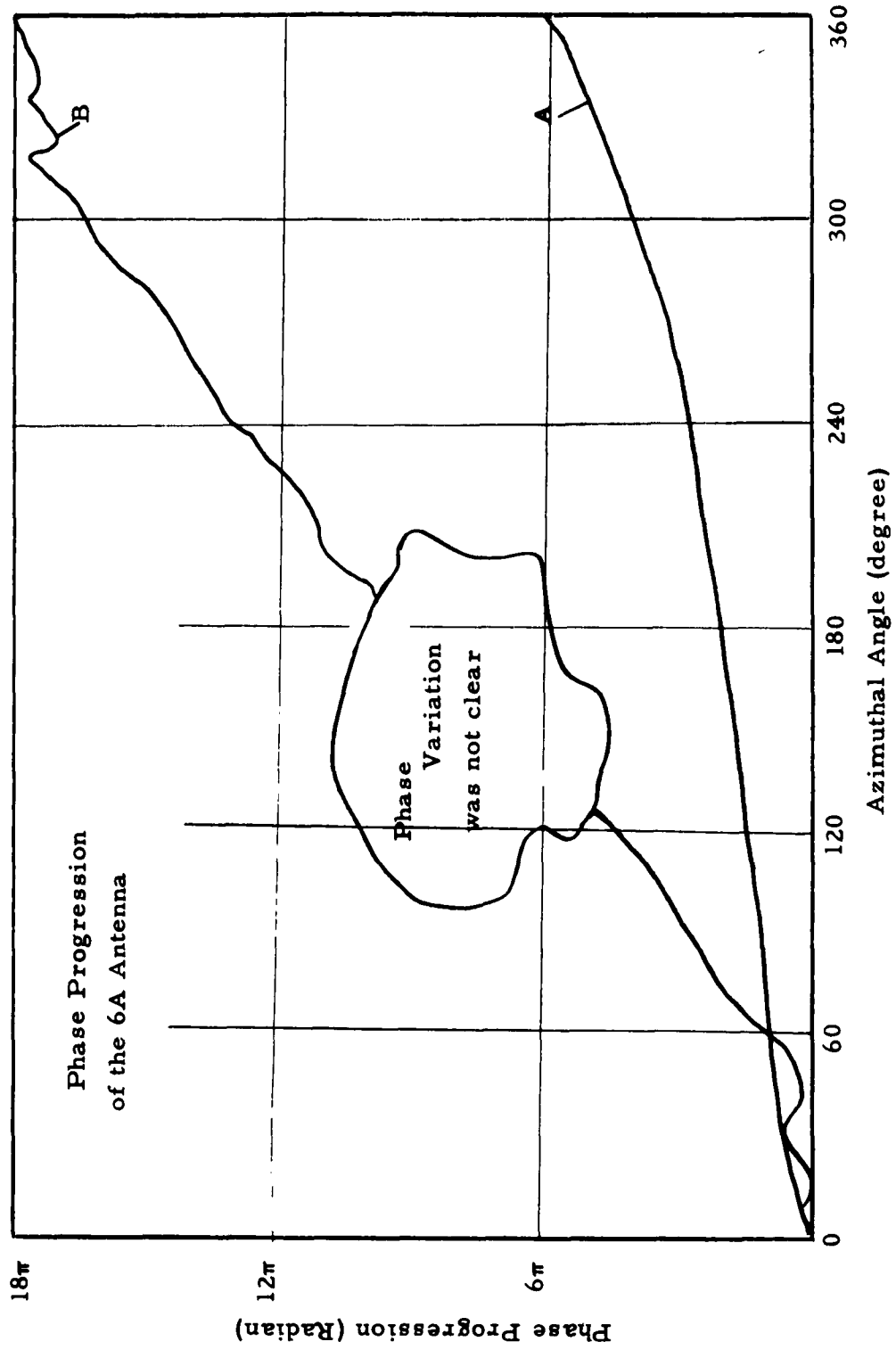


Fig. 31. -- The phase progression of the 6A-antenna as a function of the azimuthal angle, (see Sec. III, H), when fed by the I_3 characteristic feeding. Curve A: measurements taken in region II. Curve B: measurements taken in region III.

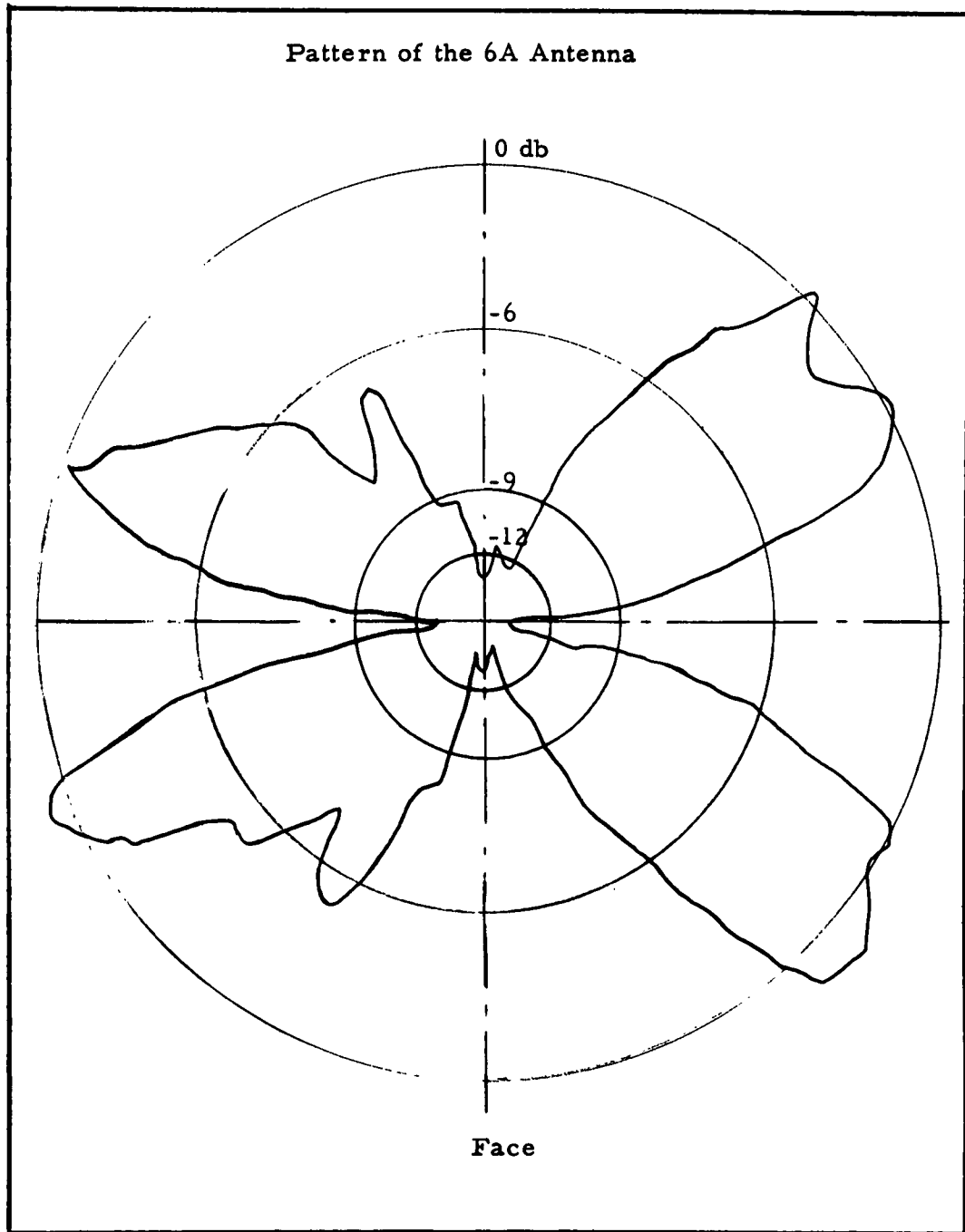


Fig. 32. --The pattern of the 6A-Antenna as measured in a plane perpendicular to the plane of the antenna through its axis, with a horn serving as receiving antenna.

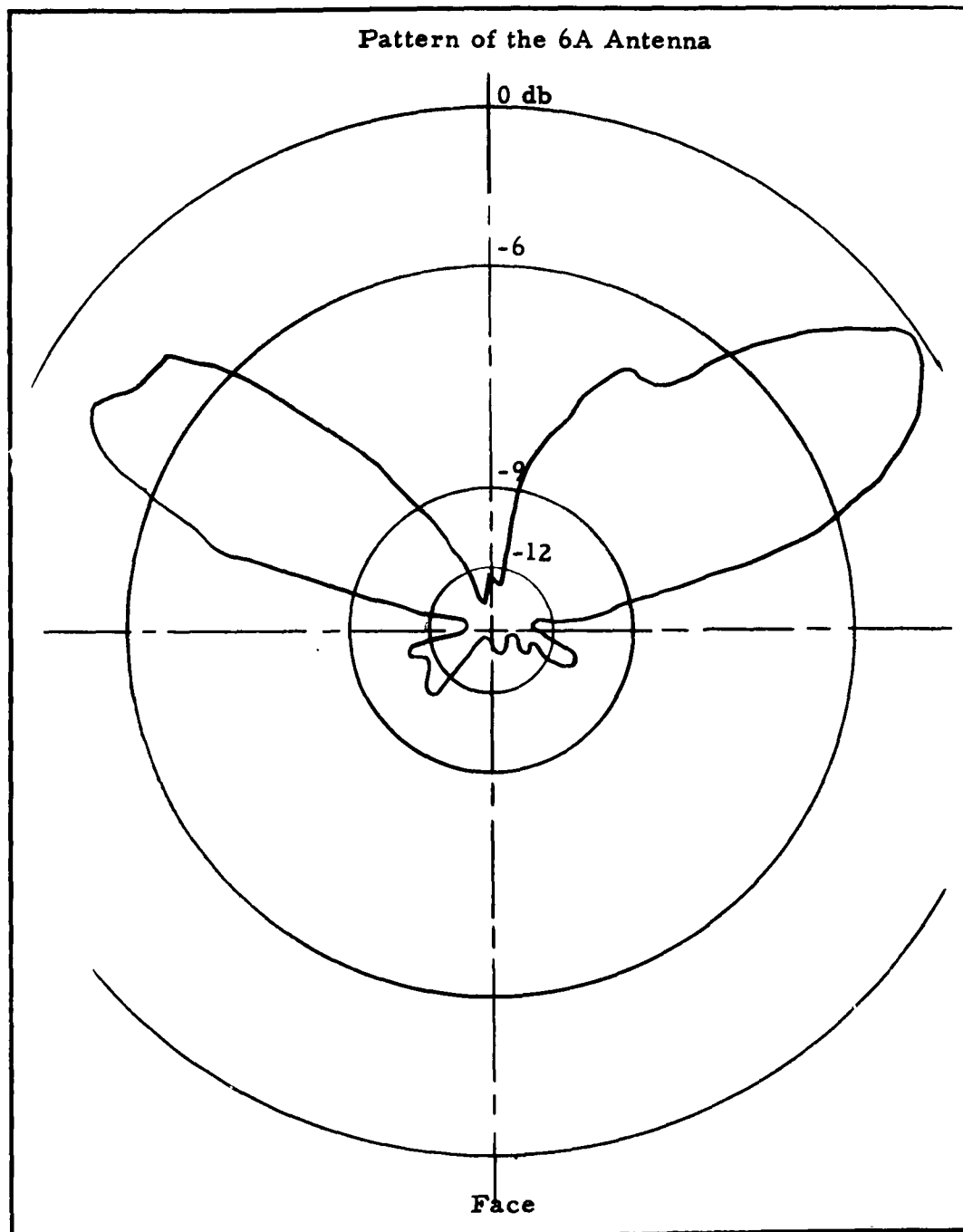


Fig. 33. --The pattern of the 6A-Antenna as measured in a plane perpendicular to the plane of the antenna through its axis, with a helix serving as receiving antenna.

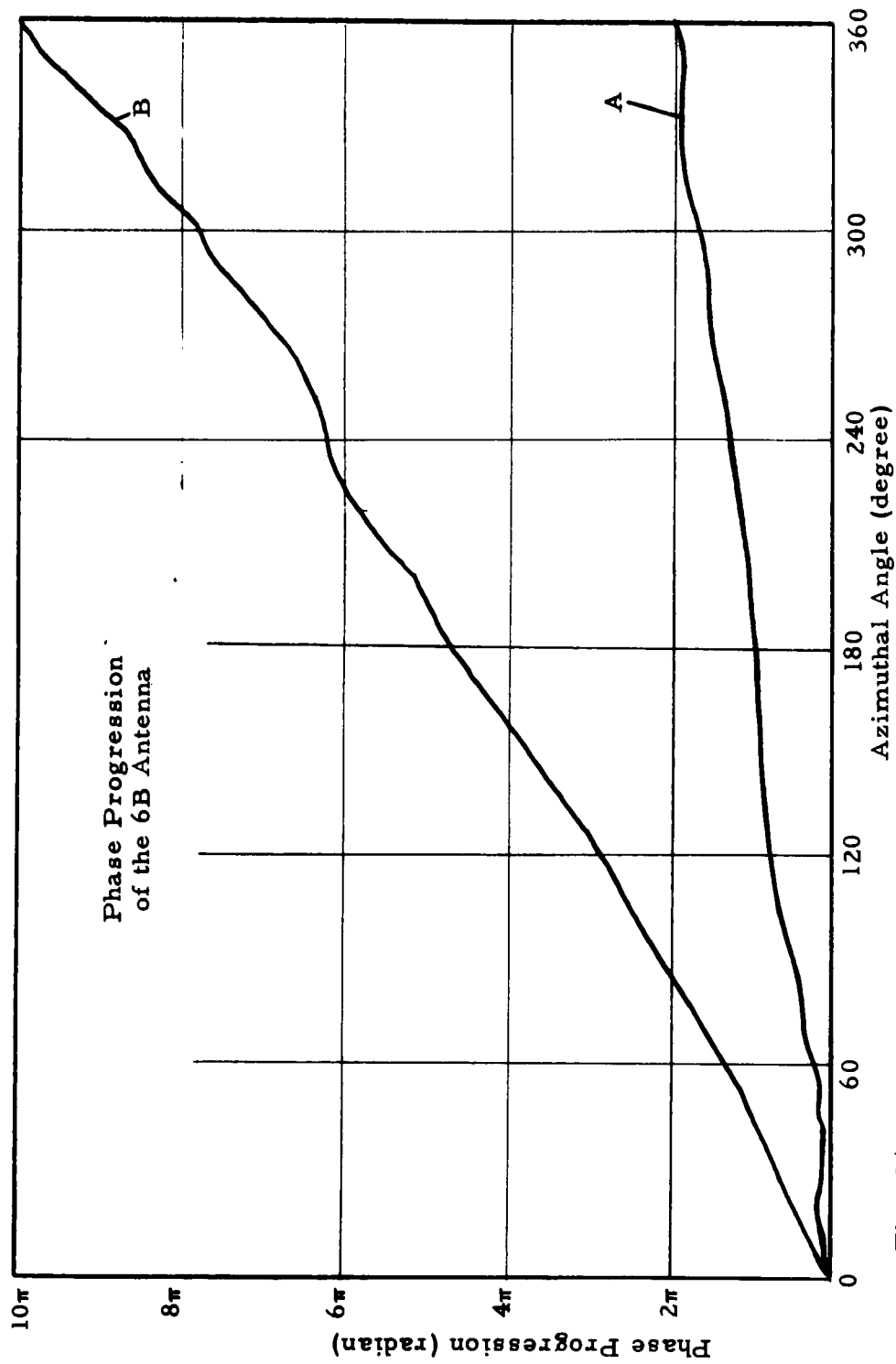


Fig. 34. -- The phase progression of the 6B-Antenna as a function of the azimuthal angle, (see Sec. III, I).
 Curve A: measured in the inner part of region II, (less than 3 cm off the axis).
 Curve B: measured in the outer part of region II, (more than 3 cm off the axis).

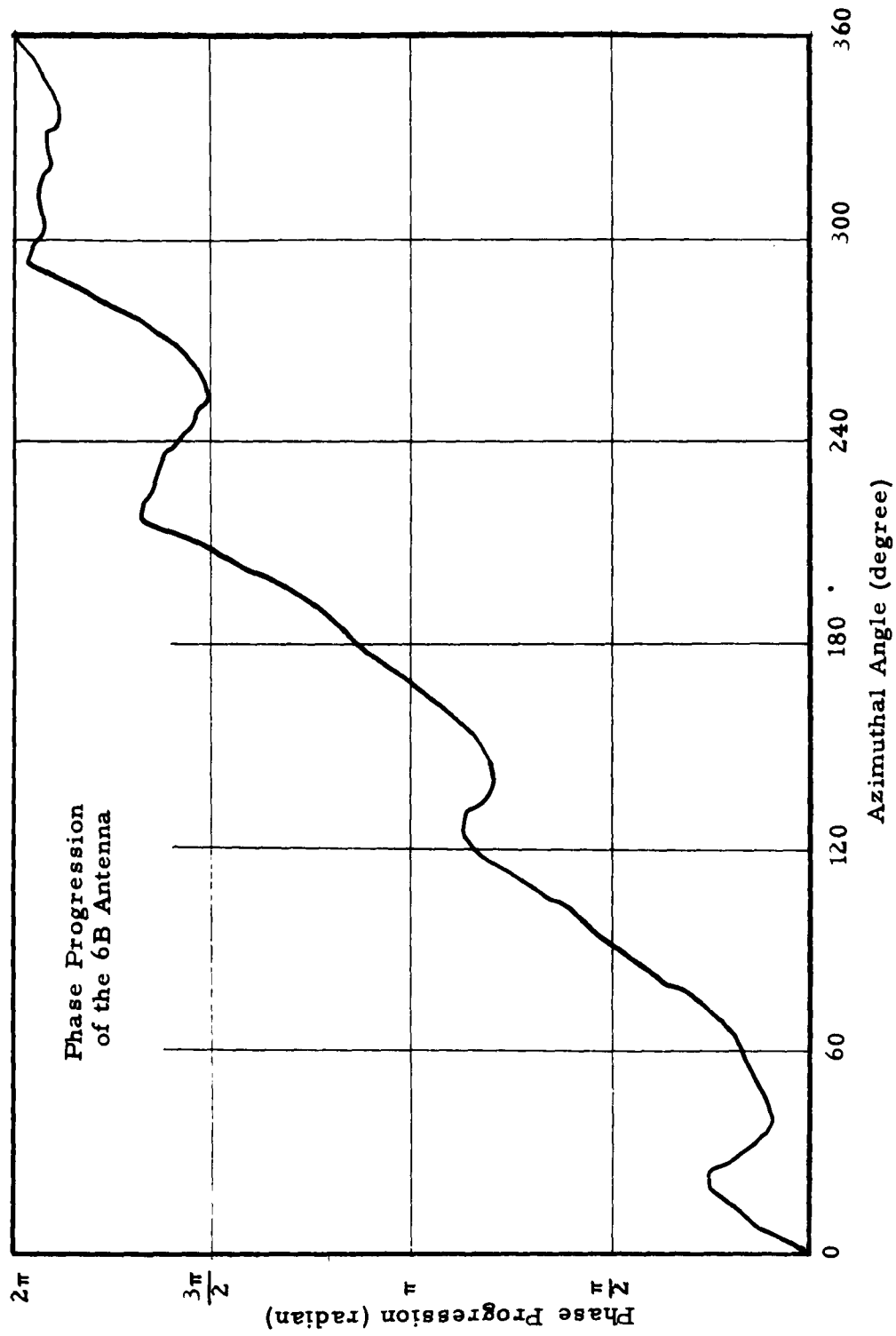


Fig. 35. -- The phase progression of the 6B-Antenna as a function of the azimuthal angle, (See Ch. III, I), as measured on the border between the inner and the outer part of region II, (4 cm off the axis).

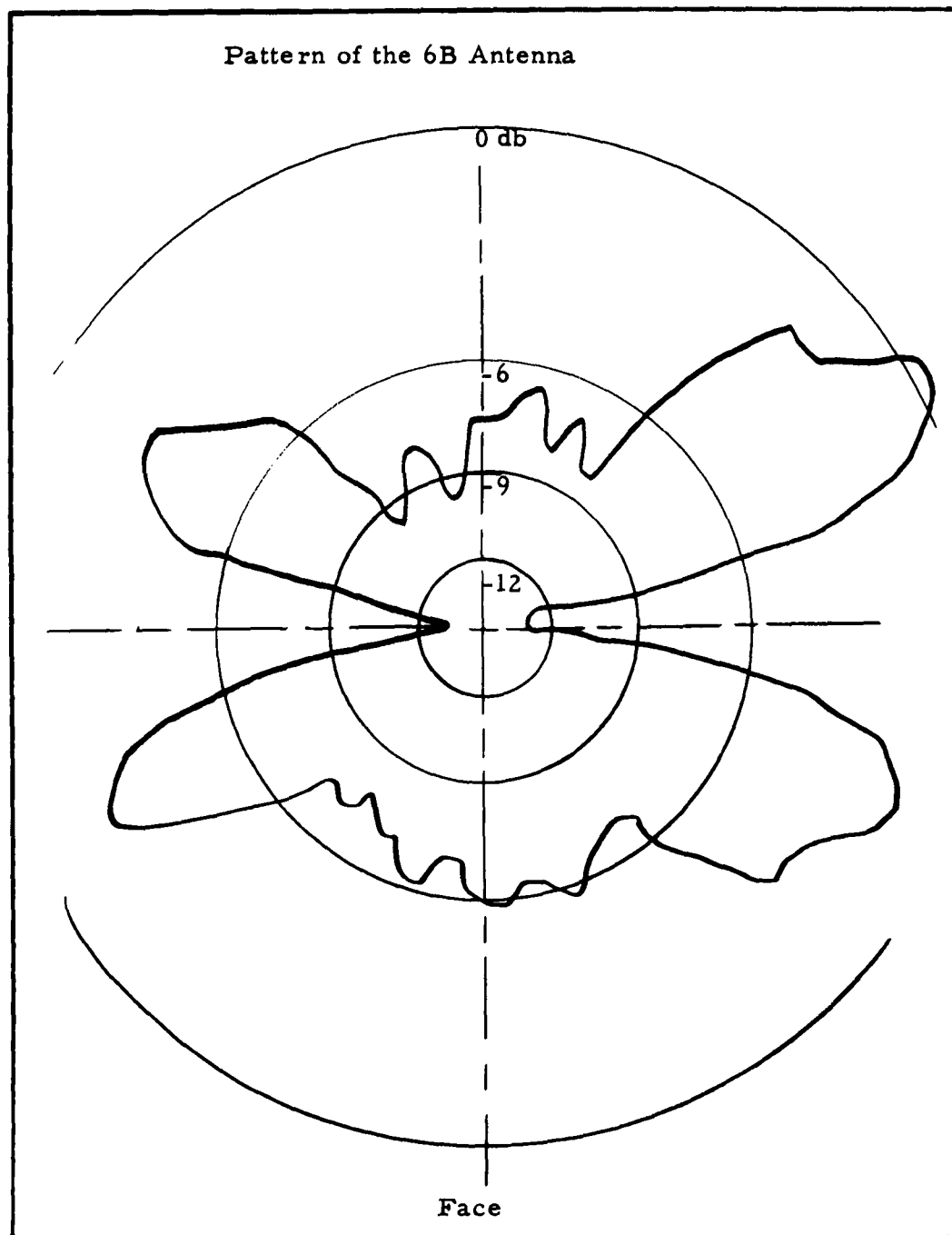


Fig. 36. --The pattern of the 6b-Antenna as measured in a plane perpendicular to the plane of the antenna through its axis, with a horn serving as receiving antenna.

The Antenna	2A	4A	4B	4C	6A	6B
The feeding arrangement						
The characteristic feeding	$2I_1$	$4I_2$	$4I_1$	$4I_1 + 4I_3$	$6I_3$	$6I_1 + 6I_5$
The Phase Variation	Region I	2π	2π	2π	6π	2π
	Region II	2π	2π	2π	6π	2π
	Region III		12π		18π	10π
The Pattern						
The Polarization						
+ preferred sense	+	+	+	+	+	+
- unpreferred sense			-			

Fig. 37. --A summarized table of the measurements.

REFERENCES

1. V. H. Rumsey, "Frequency Independent Antennas," IRE Conv. Rec., 1957
2. B. R. Cheo, "A Solution to the Equiangular Spiral Antenna Problem," Electronics Res. Lab., Univ. of California, Berkeley, Series No. 60, Issue No. 324, Nov. 1, 1960.
3. G. A. De Champs, IRE, Trans. on Ant. and Prop., Dec. 1959.
4. H. G. Booker, JIEE, part III-A, pp. 620-627, March-May 1946.
5. J. D. Dyson, The Tenth Annual Symposium on the USAF Antenna Research and Development Program, Univ. of Illinois, Oct. 3, 1960.

DISTRIBUTION LIST
AF 49(638)-1043

ORGANIZATION	NO. COPIES	ORGANIZATION	NO. COPIES	ORGANIZATION	NO. COPIES	ORGANIZATION	NO. COPIES
Advanced Research Projects Agency Washington 25, D. C.	1	Commander, Detachment 1 Naval Air Force Research Division The Shell Building Brussels, Belgium	2	P. O. Box AA Wright-Patterson Air Force Base Ohio	1	Chief, Bureau of Aeronautics Navy Department Washington 25, D. C. Attn: EL-51	1
Aeronautical Research Laboratories Attn: Technical Library, Bldg. 450 Wright-Patterson Air Force Base Ohio	1	Commander Rome Air Development Center Attn: RAWLD Griffis Air Force Base Rome, New York	1	RCA Laboratories Princeton, New Jersey Attn: Dr. W. M. Webster, Director Electronics Research Laboratories	1	Chief, Bureau of Ships Navy Department Washington 25, D. C. Attn: Code 436	2
Applied Mechanics Reviews Southwest Research Institute 8500 Culebra Road San Antonio 9, Texas	1	Commander Wright Air Development Division Attn: WWAD Wright-Patterson Air Force Base Ohio	4	Dr. Irving Rowe Office of Naval Research 146 Broadway New York, New York	1	Chief of Naval Research Navy Department Washington 25, D. C. Attn: Code 427	2
ARO, Inc. Attn: AEDC Library Arnold Air Force Station Tullahoma, Tennessee	1	Commanding General U. S. Army Signal Corps Research and Development Laboratory Attn: SIGFM/EL-RPO Fort Monmouth, New Jersey	1	Sylvania Electric Company Mountain View, California Attn: D. H. Goodman	1	Chief of Naval Research Navy Department Washington 25, D. C. Attn: Code 460	1
ASTIA Attn: TIPCR Arlington Hall Station Arlington 12, Virginia	10	Director, Army Research Office Attn: Scientific Information Branch Department of the Army Washington 25, D. C.	1	Technical Information Libraries Bell Telephone Laboratories, Inc. Whippany Laboratory Whippany, New Jersey Attn: Technical Reports Librarian	1	Commander Air Force Office of Scientific Research Air Research and Development Command Washington 25, D. C.	1
Prof. N. Huenberger Department of Physics Harvard University Cambridge 38, Massachusetts	1	Director, Department of Commerce Office of Technical Services Washington 25, D. C.	1	University of Illinois Department of Electrical Engineering Urbana, Illinois Attn: H. Von Foerster	1	Columbia Radiation Laboratories Columbia University 518 W. 120th St. New York 27, New York Attn: Librarian	1
Prof. Harvey Brooks Department of Physics Harvard University Cambridge 38, Massachusetts	1	Director, Naval Research Laboratory Attn: Technical Information Officer Washington 25, D. C.	1	The University of Michigan Department of Electrical Engineering Electron Physics Laboratory Ann Arbor, Michigan Attn: Prof. J. E. Rowe	1	Commander Naval Air Development Center Johnsville, Pennsylvania Attn: AEEL	1
Chairman, Canadian Joint Staff For DRB/DSIS 490 Massachusetts Ave., N.W. Washington 25, D. C.	1	Director, Office of Ordnance Research Box CM, Duke Station Durham, North Carolina	1	U. S. Atomic Energy Commission Technical Information Extension P. O. Box 96 Oak Ridge, Tennessee	1	Commander U. S. Naval Electronics Laboratory San Diego, California	1
Chief, Physics Branch Division of Research U. S. Atomic Energy Commission Washington 25, D. C.	1	Director of Research and Development Headquarters USAF Attn: AFDRD Washington 25, D. C.	1	Varian Associates All Hansen Way Palo Alto, California Attn: Technical Library	1	Commanding General Rome Air Development Center Griffis Air Force Base Rome, New York Attn: RCRW	1
Commandant Air Force Institute of Technology (AU) Library, MCL-LIB, Bldg. 124, Area B Wright-Patterson Air Force Base Ohio	1	General Electric Company Electron Tube Division of the Research Laboratory The Knolls Schenectady, New York Attn: E. D. McArthur	1	Westinghouse Electric Corp. Electronic Tube Division P. O. Box 484 Elmira, New York Attn: Mr. Sheldon S. King, Librarian	1	Commanding General Signal Corps Engineering Laboratories Evans Signal Laboratory Area Building 47 Belmont, New Jersey Attn: Technical Documents Center	1
Commander Air Force Cambridge Research Laboratories Attn: CRREL 1, G. Hanscom Field Bedford, Massachusetts	1	Dr. Harold Glaser Office of Naval Research Washington 25, D. C.	1	M. D. Adcock, Head Microwave Systems and Components American Systems, Inc. 1412 Century Boulevard Inglewood, California	1	Commanding General Signal Corps Engineering Laboratories Fort Monmouth, New Jersey Attn: SIGEL-SMB-md, MOB-Magnetic Materials	1
Commander Air Force Flight Test Center Attn: FTOTL Edwards Air Force Base California	1	Harvard University Cruft Laboratory Cambridge 38, Massachusetts Attn: Technical Reports Collection	1	Antenna Laboratory Ohio State University Research Foundation Columbus, Ohio Attn: Dr. C. T. Tai	1	Commanding General Wright Air Development Center Wright-Patterson Air Force Base Ohio Attn: WCRCO-2	1
Commander Air Force Missile Development Center Attn: HDO Holloman Air Force Base New Mexico	1	Hughes Aircraft Company Florence at Teale St Culver City, California Attn: Documents Group, Bldg. 6, Rm. X2015	1	Assistant Secretary of Defense Research and Development Board Department of Defense Washington 25, D. C.	1	Department of Electrical Engineering Cornell University Ithaca, New York Attn: Dr. H. G. Booker	1
Commander Air Force Office of Scientific Research Attn: SRY Washington 25, D. C.	3	Institute of Aeronautical Sciences Attn: Librarian 2 East 64 St. New York 17, New York	1	Bell Telephone Laboratories, Inc. Central Serial Records Technical Information Library 463 West St. New York 14, New York	1	Department of Electrical Engineering Yale University New Haven, Connecticut	1
Commander Air Force Research Division Attn: RRRTL Washington 25, D. C.	2	Prof. Zohrab Kaprielian University of Southern California School of Engineering Department of Electrical Engineering University Park Los Angeles 7, California	1	Boeing Aircraft Company Physical Research Unit Seattle 14, Washington Attn: Mr. E. W. Hillman	1	Director, Naval Research Laboratory White Oak, Maryland	1
Commander Air Force Special Weapons Center Attn: SWOC Kirtland Air Force Base New Mexico	1	Prof. P. Kusch Department of Physics Columbia University New York 27, New York	1	Dr. C. J. Bouwkamp Phillips Research Laboratories N. V. Phillips Glowlampfabrieken Eindhoven, Netherlands VIA ONR London	1	Director, Naval Research Laboratory Washington 25, D. C. Attn: Code 5250	1
Commander Air Research and Development Command Attn: RDR Andrews Air Force Base Washington 25, D. C.	2	Massachusetts Institute of Technology Research Laboratories of Electronics Room 40B-221 Document Office Cambridge 39, Massachusetts Attn: J. H. Hewitt	1	Douglas Aircraft Co., Inc El Segundo Division El Segundo, California	1	Douglas Aircraft Co., Inc El Segundo Division El Segundo, California	1
Commander Air Research and Development Command Attn: RDR Andrews Air Force Base Washington 25, D. C.	1	Hans Motz Oxford University Oxford, England	1	Electrical Engineering Department Illinois Institute of Technology Technology Center Chicago 16, Illinois	1	Electrical Engineering Department University of Texas Box F, University Station Austin, Texas	1
Commander Air Research and Development Command Attn: RDR Andrews Air Force Base Washington 25, D. C.	1	National Aeronautics and Space Administration Washington 25, D. C.	1	California Institute of Technology Pasadena, California Attn: C. H. Pappas	1	Electronics Research Laboratory Stanford University Stanford, California Attn: Applied Electronics Laboratory Documents Library	1
Commander Air Research and Development Command Attn: RDR Andrews Air Force Base Washington 25, D. C.	1	National Bureau of Standards Library Room 203, Northwest Building Washington 25, D. C.	1	Cambridge University Radiophysics Division Cavendish Laboratory Cambridge, England VIA ONR London	1	Federal Telecommunications Laboratories, Inc. 506 Washington Ave. Nutley, New Jersey Attn: A. K. Wing	1
Commander Air Research and Development Command Attn: RDR Andrews Air Force Base Washington 25, D. C.	1	Office of Naval Research Department of the Navy Attn: Code 420 Washington 25, D. C.	1	Chalmers Institute of Technology Göteborg, Sweden VIA ONR London	1		
Commander Air Research and Development Command Attn: RDR Andrews Air Force Base Washington 25, D. C.	1	Ohio State University Department of Electrical Engineering Columbus, Ohio	1				
Commander Air Research and Development Command Attn: RDR Andrews Air Force Base Washington 25, D. C.	1	Mr. E. Okress Sperry Gyroscope Company Electron Tube Division Mail Station 1B10 Great Neck, New York	1				
Commander Army Rocket and Guided Missile Agency Attn: ORDR OTL Redstone Arsenal Alabama	1	Physics Program National Science Foundation Washington 25, D. C.	1				

ORGANIZATION	NO. COPIES	ORGANIZATION	NO. COPIES	ORGANIZATION	NO. COPIES
Georgia Institute of Technology Atlanta, Georgia Attn: Mrs. J. Fenley Crosland, Librarian	1	Technical University Department of Electrical Engineering Delft, Holland VIA ONR London Attn: Prof. J. P. Schouten	1	Commanding Officer U.S. Army Signal Research and Development Laboratory Fort Monmouth, New Jersey Attn: Technical Documents Center	1
Carl A. Hedberg, Head Electronics Division Denver Research Institute University of Denver Denver, Colorado	1	University of Florida Gainesville, Florida Attn: Applied Electronics Laboratory Document Library	1	Commanding Officer U.S. Army Signal Research and Development Laboratory Fort Monmouth, New Jersey Attn: SIGRA/SL-PRM (Records File Copy)	1
Hughes Aircraft Company Antenna Research Department Bldg. 12, Room 2617 Culver City, California	1	U.S. Naval Post Graduate School Monterey, California Attn: Librarian	1	Commanding Officer U.S. Army Signal Research and Development Laboratory Fort Monmouth, New Jersey Attn: Logistics Division (For SIGRA/SL-PRM) (Project Engineer)	2
Hughes Aircraft Company Research and Development Library Culver City, California Attn: John T. Milek	1	Watson Laboratories Library AMC, Red Bank, New Jersey Attn: ENAGSI	1	Commanding Officer U.S. Army Signal Research and Development Laboratory Fort Monmouth, New Jersey Attn: Technical Information Division 5 (FOR RETRANSMITTAL TO ACCREDITED BRITISH AND CANADIAN GOVERNMENT REPRESENTATIVES AND TO DEPARTMENT OF COMMERCE)	5
Library Boulder Laboratories National Bureau of Standards Boulder, Colorado Attn: Victoria S. Barker	2	Willow Run Research Center University of Michigan Ypsilanti, Michigan Attn: Dr. K. Siegel	1	Deputy President U.S. Army Security Agency Board Arlington Hall Station Arlington 12, Virginia	1
Mathematics Research Group New York University 25 Waverly Place New York, New York Attn: Dr. M. Kline	1	Advisory Group on Electron Tubes 346 Broadway New York 13, New York Attn: Dr. W. Kluver	2	Director, U.S. Naval Research Laboratory Washington 25, D. C. Attn: Code 2027	1
Mr. Frank J. Mullin Department of Electrical Engineering California Institute of Technology Pasadena, California	1	Bell Telephone Laboratories Murray Hill, New Jersey Attn: Dr. W. Kluver	1	The European Office U.S. Army R and D Liaison Group APO 757 New York, New York (FOR RETRANSMITTAL TO CONTRACTOR, DA 91-591-EUC-1312)	1
Naval Air Missile Test Center Point Mugu, California	1	California Institute of Technology Electron Tube and Microwave Laboratory Pasadena, California Attn: Prof. R. Gould	1	Hughes Aircraft Company Culver City, California Attn: Dr. Mendel, Microwave Tube Laboratory	1
Office of the Chief Signal Officer Pentagon Washington 25, D. C. Attn: SIGET	1	Chief, Bureau of Ships Department of the Navy Washington 25, D. C. Attn: 691A4	1	Marine Corps Liaison Office U.S. Army Signal Research and Development Laboratory Fort Monmouth, New Jersey	1
Office of Technical Services Department of Commerce Washington 25, D. C.	1	Chief of Ordnance Washington 25, D. C. Attn: ORDTX-AR	1	Massachusetts Institute of Technology Research Laboratory of Electronics Cambridge, Massachusetts Attn: Prof. L. Smullin	1
Radiation Laboratory Johns Hopkins University 1315 St. Paul St. Baltimore 2, Maryland Attn: Librarian	1	Chief of Research and Development OCS, Department of the Army Washington 25, D. C.	1	OASD (R and E), Rm. 3E1065 The Pentagon Washington 25, D. C. Attn: Technical Library	1
The Rand Corporation 1700 Main St. Santa Monica, California Attn: Margaret Anderson, Librarian	1	Chief Signal Officer Department of the Army Washington 25, D. C. Attn: SIGRD	1	Radio Corporation of America Laboratories Princeton, New Jersey Attn: Dr. L. S. Nergaard	1
Randall Morgan Laboratory of Physics University of Pennsylvania Philadelphia 4, Pennsylvania	1	Chief, U.S. Army Security Agency Arlington Hall Station Arlington 12, Virginia	2	Raytheon Manufacturing Company Microwave and Power Tube Operations Waltham 54, Massachusetts Attn: W. C. Brown	1
Regents of the University of Michigan Ann Arbor, Michigan	1	Commander Air Force Command and Control Development Division Air Research and Development Command United States Air Force Laurence G. Hanscom Field Bedford, Massachusetts Attn: CROTL	1	Research Division Library Raytheon Company 28 Seyon St. Waltham 54, Massachusetts	1
Research Laboratory of Electronics Document Room Massachusetts Institute of Technology Cambridge 39, Massachusetts Attn: Mr. J. Hewitt	1	Commander Wright Air Development Division Attn: WCOSI-3 Wright-Patterson Air Force Base Ohio	2	S. F. D. Laboratories, Inc. 800 Rahway Ave. Union, New Jersey	1
Prof. Vincent C. Rideout Department of Electrical Engineering University of Wisconsin Madison 6, Wisconsin	1	Commanding Officer Diamond Ordnance Fuse Laboratories Washington 25, D. C. Attn: Library, Rm. 211, Bldg. 92	1	Stanford University Electronic Research Laboratory Palo Alto, California Attn: Prof. D. A. Watkins	1
Royal Technical University Laboratory for Telephony and Telegraphy Ostervoldgade 10 Copenhagen, Denmark VIA ONR London Attn: Prof. H. L. Knudsen	1	Commanding Officer Frankford Arsenal Philadelphia 37, Pennsylvania Attn: ORDBA-FEL	1	Sylvania Electric Products Physics Laboratory Bayside, Long Island, New York Attn: L. R. Bloom	1
Prof. Samuel Seely, Head Department of Electrical Engineering Case Institute of Technology University Circle Cleveland 6, Ohio	1	Commanding Officer and Director U.S. Navy Electronics Laboratory San Diego 52, California	1	U.S. Navy Electronics Liaison Office U.S. Army Signal Research and Development Laboratories Fort Monmouth, New Jersey	1
Signal Corps Engineering Laboratories Fort Monmouth, New Jersey Attn: Mr. O. C. Woodyard	1	Commanding Officer 9560th TSU U.S. Army Signal Electronics Research Unit P. O. Box 205 Mountain View, California	1	Watkins-Johnson Company 333 Hillview Ave. Stanford Industrial Park Palo Alto, California	1
Stanford Research Institute 974 Commercial Stanford, California Attn: Dr. John T. Bolljohn Division of Electrical Engineering	1	Commanding Officer U.S. Army Signal Material Support Agency Attn: SIGMS-ADJ	1	Westinghouse Electric Corporation Research Laboratory Beulah Road, Churchill Boro Pittsburgh 35, Pennsylvania	1
Technical Reports Collection 303A Pierce Hall Harvard University Cambridge 38, Massachusetts	1	Commanding Officer U.S. Army Signal Research and Development Laboratory Fort Monmouth, New Jersey Attn: Director of Research	1		
		Commanding Officer Office of Naval Research, Branch Office 1000 Geary St. San Francisco 9, California	1		